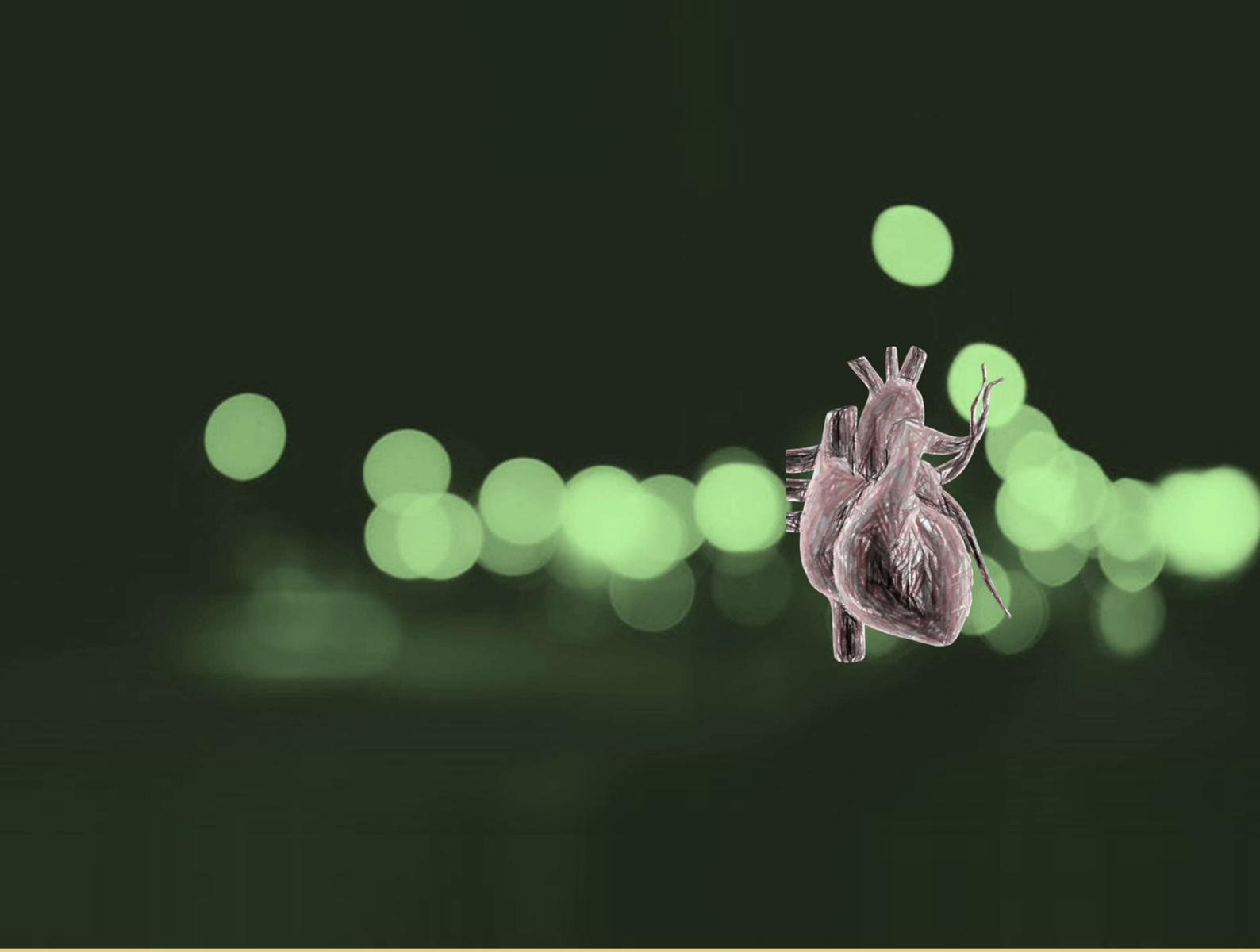

Alexandre Manuel Monteiro Gonçalves

T3 Hormone as an effective therapy for Heart Failure with Preserved Ejection Fraction: Effects on Ca^{2+} transients and contractility

Master Dissertation in Biomedical Research – Cardiovascular Sciences
presented to the Faculty of Medicine of the University of Coimbra

April 2018

· U C ·

UNIVERSIDADE DE COIMBRA

FMUC FACULDADE DE MEDICINA
UNIVERSIDADE DE COIMBRA

Alexandre Manuel Monteiro Gonçalves

T3 HORMONE AS AN EFFECTIVE THERAPY FOR HEART FAILURE WITH PRESERVED EJECTION FRACTION: Effects on Ca^{2+} transients and contractility

Alexandre Manuel Monteiro Gonçalves

HORMONA T3 COMO UMA TERAPIA EFETIVA PARA INSUFICIENCIA CARDIACA COM FRAÇÃO DE EJEÇÃO PRESERVADA: Efeitos nos transientes de Ca^{2+} e contractilidade

Dissertação apresentada à Faculdade de Medicina da Universidade de Coimbra para cumprimento dos requisitos necessários à obtenção do grau de Mestre em Investigação Biomédica – Ciências Cardiovasculares, realizada sob orientação científica da Prof. Drª Inês Falcão Pires, Investigadora Principal/Professora Auxiliar na Faculdade de Medicina do Porto e do Prof. Dr. Henrique Girão, Investigador Principal/Professor Auxiliar na Faculdade de Medicina da Universidade de Coimbra.

Alexandre Manuel Monteiro Gonçalves

T3 HORMONE AS AN EFFECTIVE THERAPY FOR HEART FAILURE WITH PRESERVED EJECTION FRACTION: Effects on Ca^{2+} transients and contractility

Dissertation presented to the Faculty of Medicine of the University of Coimbra to comply with the requirements necessary for the degree of Master in Biomedical Research – Cardiovascular Sciences, under the scientific orientation of Prof. Inês Falcão Pires, Principal Investigator/Assistant Professor in the Faculty of Medicine at the University of Porto and Prof. Henrique Girão, Principal Investigator/Assistant Professor in the Faculty of Medicine at the University of Coimbra.

Host Institution

Departamento de Cirurgia e Fisiologia

Unidade de Investigação Cardiovascular

Centro de Investigação Médica, 6º piso

Faculdade de Medicina da Universidade do Porto

Rua Dr Plácido da Costa

4200-450 Porto, Portugal

Supervisor: Inês Falcão-Pires, PhD[1]

Co-supervisor: Henrique Girão, PhD[2]

Affiliations:

[1] FMUP - Faculdade de Medicina da Universidade do Porto

[2] FMUC - Faculdade de Medicina da Universidade de Coimbra

Agradecimentos /

Acknowledgments

This master dissertation marked the start of my first delve into the complex field that is a more physiology-oriented scientific research, as someone that, until very recently, only had contact with basic molecular research. Needless to say, that it all came as a strong complement to my intentions of developing translational research with direct clinical relevance.

As such, firstly, I would like to express gratitude towards Professor Adelino Leite Moreira for giving me this opportunity and always being available to discuss and advise whenever needed.

To my supervisor, Professor Inês Falcão Pires, I would like to express my sincere thanks for the warm welcome into her group, continuous support, her immense knowledge and guidance.

I would also like to acknowledge Professor Henrique Girão, for all the help throughout the years and for promoting my academic growth.

A special acknowledgement to João Neves for allowing me to be part of his project and always being available to discuss results.

Finally, I must express my very profound gratitude towards all my fellow lab colleagues, especially Daniela Silva, Dulce Fontoura, Glória Conceição, João Coelho, S. Marisa Oliveira and Nádia Gonçalves for all the help, stimulating discussion and for the company in the sleepless nights in the lab.

I hereby formally thank the University of Porto, my host institution, for providing me the facilities to conduct this dissertation and the University of Coimbra for the support in this endeavor.

But most of all, I would like to express my gratefulness to Comboios de Portugal, for their constant delays in both departures and trip durations that fashioned the boring and monotonous ambient ideal for reading articles and writing the dissertation.

Palavras-chave

Cardiomiócitos isolados; FURA-2; Medições de contractilidade; Insuficiência cardíaca com fração de ejeção preservada (ICFEP); Triiodotironina (T3); Tiroide; Terapia;

Resumo

A insuficiência cardíaca com fração de ejeção preservada (ICFEP) constitui um frequente problema clínico, mas até hoje, nenhuma intervenção terapêutica parece modular o seu desfecho clínico. Alguns doentes com ICFEP possuem alterações no eixo hormonal da tiroide e é já conhecido o impacto da influência destas hormonas sobre o sistema cardiovascular. Neste projeto, testamos a hipótese de que administração oral preventiva com triiodotironina (T3) pode prevenir o desenvolvimento de ICFEP.

Iniciou-se às 14 semanas de idade a administração oral de T3 (0.04 - 0.06 µg/mL) ou veículo em ratos ZSF1 obesos (ICFEP), utilizando ratos ZSF1 magros (CT) como controlo. A função tiroideia foi avaliada através de medições dos níveis plasmáticos de T3, T4 e TSH a cada 2 semanas e a dose de T3 administrada ajustada. No final do protocolo (24 semanas), foi realizada a avaliação ecocardiográfica, hemodinâmica e morfométrica dos animais. Os corações foram recolhidos e perfundidos enzimaticamente para isolamento de cardiomiócitos de forma a medir a contractilidade e a cinética dos transientes de Ca^{2+}, usando a sonda fluorescente FURA-2.

Cardiomiócitos isolados de ratos ICFEP apresentaram disfunção inotrópica e lusitrópica relativamente ao CT tal como observado pela diminuição na amplitude de contração, aumento no tempo até ao pico de contração e de relaxamento. A suplementação com T3 mostrou-se efetiva a normalizar a função. A maiores frequências de estimulação, a concentração de Ca^{2+} citoplasmático aumentou significativamente, mas o tratamento com T3 provou prevenir essa subida.

Estes resultados constituem uma base de evidência promissora para os benefícios que a suplementação de T3 tem num subtipo particular de doentes com ICFEP com evidência de hipotiroidismo.

Keywords

Isolated Cardiomyocytes; FURA-2; Contractility measurements; Heart Failure with Preserved Ejection Fraction (HFpEF); Triiodothyronine (T3); Thyroid; Therapy;

Abstract

Heart failure with preserved ejection fraction (HFpEF) constitutes a major clinical problem, but to this day no therapy has effectively changed the course of the disease. Some HFpEF patients have alterations in the thyroid hormonal axis, and these hormones are known to influence cardiac function. In this project, we tested the hypothesis that preemptive triiodothyronine (T3) oral administration can prevent HFpEF development.

Beginning at 14 weeks of age, ZSF1 obese rats (HFpEF) were orally administered with T3 (0.04 - 0.06 µg/mL) or vehicle, using ZSF1 lean rats (CT) as a control. Thyroid function was assessed through T3, T4 and TSH serum levels every two weeks and the dose was adjusted accordingly. At the end of the protocol (24 weeks), animals were evaluation by echocardiography, hemodynamics and morphometrics. The hearts were removed and enzymatically perfused to isolate cardiomyocytes for contractility and Ca^{2+} transient kinetics measurements using the FURA-2 fluorescent probe.

Cardiomyocytes isolated from HFpEF rats shown inotropic and lusitropic impairments, as assessed by decreased contractile amplitude, increased time to peak contraction and relaxation, when compared to CT. T3 supplementation was found to be effective at normalizing these parameters. Higher stimulation frequencies led to cytoplasmic Ca^{2+} accumulation in HFpEF rat cardiomyocytes, while T3 treatment prevented this.

These results constitute promising findings supporting the benefits of T3 supplementation in a certain subtype of HFpEF patients with evidence of hypothyroidism.

Contents

List of Figures

List of Tables

List of Abbreviations

BNP	-	B-type Natriuretic Peptide
BW	-	Body Weight
CVD	-	Cardiovascular Disease
FURA-2 AM	-	FURA-2 Acetoxymethyl
HF	-	Heart Failure
HFpEF	-	Heart Failure with Preserved Ejection Fraction
IVC	-	Isolated Ventilated Cage
IR	-	Insulin Resistance
LV	-	Left Ventricle
PLB	-	Phospholamban
RCP	-	Retrograde Coronary Perfusion
TH	-	Thyroid Hormone
TSH	-	Thyroid Stimulating Hormone
T3	-	Triiodothyronine
T4	-	Thyroxine
ZSF1	-	Zucker fatty / Spontaneously Hypertensive Heart Failure F1 Hybrid

Chapter 1

Introduction

Cardiovascular disease (CVD) has always occupied a place at the center stage of medical complications. The evolution towards an ever-aging population, in addition to increased risk factors, such as poor diet and lack of exercise, have come to further cemented its place as the leading cause of death worldwide. In 2013 alone, 31.5% of all global deaths were attributed to CVD[1] and, by 2020, according to the World Health Organization, these numbers tend to aggravate[2].

Heart Failure (HF) represents a major public health issue, affecting 23 million people worldwide[3]. With a lifetime risk of approximately 31%, according to the most recent ESC guidelines[4], and a 5-year mortality rate that challenges those of many cancers[3], the global panorama seems dire.

The terminology HF encompasses a wide range of patients that are sorted according to the measurement of left ventricular ejection fraction. One of these sub-types of HF, Heart Failure with Preserved Ejection Fraction (HFpEF), underlined by anomalies in left ventricular relaxation and stiffness, now represents over 50 % of HF cases[1,3,5] and is reported to have outcomes as poor as those associated with HF with Reduced Ejection Fraction (HFrEF)[6–8]. Additionally, unlike the latter, HFpEF remains without a single proven therapy that is accepted by the medical community or validated in clinical trials[6,9,10]. To this day, the recommendations in the European guidelines are restricted to targeting the comorbidities to ameliorate the patient well-being[4]. Several efforts were made over the years trying to reuse evidence-based drugs for HFrEF, such as β-blockers, ACE-inhibitors and mineralocorticoid antagonists, on HFpEF[11]. The results were underwhelming but served to further cement the differences in the underlying pathophysiological mechanisms of both diseases, wherein neurohumoral and sympathetic nervous systems seem to assume a critical role on HFrEF progression alone.

Despite this and all the appeals issued by the medical community, HFpEF continues to be under-researched and neglected by the scientific community, considering its prevalence and current lack of therapy[4]. This is both odd and terrifying considering HFpEF is by no means a newly discovered pathology, after all, the first report was published well over 30 years ago[12]. Figure 1 highlights this problem by providing some intriguing metrics that reflect the

asymmetry between HFpEF and HFrEF regarding the number of peer-reviewed articles published over the last 30 years.

All these problems are worrisomely manifested in clinical evidence that point towards the fact that, unlike HFrEF, HFpEF patient survival has not improved at least until 2006[13], but this trend should hold up till today.

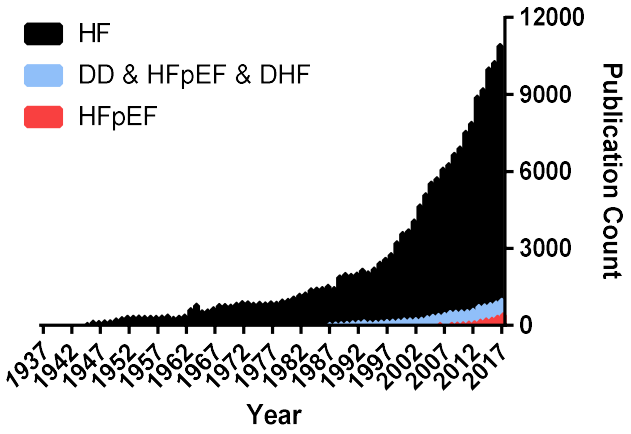

Figure 1: Heart failure with preserved ejection fraction publishing metric. Number articles indexed on PubMed obtained through the search of the following key words: **HF** = ("Heart Failure"); **DD & HFpEF & DHF** = ("diastolic dysfunction") OR ("heart failure with preserved ejection fraction") OR ("diastolic heart failure"); **HFpEF** = ("heart failure with preserved ejection fraction");
The search query was run on 19/03/2018.

HFpEF is commonly associated to diastolic dysfunction and patients have, by definition, normal or near normal ejection fraction. However, changes in systolic function are known to exist and have already been reported by tissue Doppler analysis[14,15].

Diastolic dysfunction in HFpEF is determined by increased ventricular stiffness, delayed myocardial relaxation, wall thickness and chamber geometry[16]. The mechanistic explanation for this delay is attributed to significant changes in Ca^{2+} kinetics, particularly, through diminished SERCA2 activity – the main protein responsible for Ca^{2+} reuptake into the sarcoplasmic reticulum[6]. These abnormalities ultimately lead to the hearts' inability to fill and/or eject blood that usually culminate in pulmonary and systemic venous congestion[17].

The aetiology of HFpEF is complex, but most researchers seem to agree that comorbidities take a critical role on the onset of the disease. So much so, that some have even tried to propose that HFpEF is not a disease *per se*, but a complex agglomerate of many comorbidities[18–21]. Indeed, researchers and clinicians alike tend to bundle these patients into a single entity: HFpEF. As such, one could argue that the creation of a new nomenclature that integrates the possible comorbidities known to be related to HFpEF and divides the combinations into sub-groups can provide a solid ground to improve diagnostic accuracy, providing researchers and clinicians the possibility to optimize research to these subpopulations or to personalize treatments, respectively.

Through time, researchers, trying to unravel both the mechanisms and possible therapeutic targets of HFpEF, often focused on the comorbidities. These comorbidities are not restricted to the heart, due to the multifactorial nature of the disease and thus can be of cardiovascular and non-cardiovascular origin (Table 1)[11,22].

Table 1 – HFpEF comorbidities, divided by cardiovascular (orange column) and non-cardiovascular (blue column). Less common comorbidities also shared with HFrEF are highlighted on the right column[20].

HFpEF Comorbidities		
Cardiovascular	**Non-Cardiovascular**	**Shared with HFrEF**
Hypertension	Obesity	Renal Impairement
Bradycardia	Diabetes Mellitus	Liver Disease
Pulmonary Hypertension	Aging	Peptic Ulcer Disease
Coronary Artery Disease	Gender	Hypothyroidism
Atrial Fibrillation	Chronic obstructive pulmonary disease	

HFpEF patients tend to be female, older, with history of atrial fibrillation[3] and to have higher body mass index, being more likely to be obese and often presenting with metabolic syndrome[13]. The prevalence and importance given to obesity, diabetes mellitus and hypertension in the context of this disease is high and has led to numerous studies investigating these comorbidities as valid therapeutic targets[22–25]. However, despite some promising results, none of these led to effective therapeutic options, likely due to patient heterogeneity hindering clinical studies. This resulted in a recent shifting towards focusing on ameliorating the quality of life rather than tackling the disease directly[4].

Hypothyroidism is one of the comorbidities often found in HFpEF patients, but has, for the most part, been sweeping under the radar of most researchers as a theoretical potential therapeutic target, since it is frequently underdiagnosed[26]. This is especially relevant given that the presence of hypothyroidism has already been reported to herald worse symptoms, comorbidities and overall prognosis[27].

Given the intricate nature of HFpEF, a good animal model is required to yield relevant data that can be of use as a basis in translation to human trials and further investigation. Our laboratory has recently characterized the most robust rodent animal model for HFpEF to date: the obese ZSF1 rat (ZSF1 Ob)[5]. This model develops several comorbidities associated to HFpEF, such as obesity, hypertension and diabetes mellitus. By twenty-weeks of age, the obese rats show evident markers of HFpEF, such as high filling pressures, lung congestion, impaired effort tolerance, VO_2 max, increased cardiomyocyte stiffness with preserved systolic and renal function[5,10,28].

Recent preliminary data we obtained using this animal model at twenty-weeks of age, revealed the existence of changes in the thyroid pathway, analogous to those found in humans with HFpEF. This finding was very exciting and lead us to question the effects of thyroid hormone (TH) modulation in the progression/onset of HFpEF in this animal model.

The relationship between thyroid dysfunction and cardiovascular diseases is hardly a new topic. The first description of such a case was made by William Greenfield and dates back to 1878, decades before the first TH tests became available[29,30]. By 1891, the first trial injecting

exogenous THs was carried by George Murray and shown promising results with dramatic improvements in symptomatology[31].

The cardiac tissue expresses receptors for T3[32,33] and they highly modulate its function through regulation of diverse genes (Figure 2), some intrinsically linked to calcium flux and contractile proteins[33]**.** Furthermore, T3 also has direct effects on myocardium function independent of gene modulation. These include, but are not restricted to, the activity of Ca^{2+}-ATPase, Ca^{2+} uptake by the sarcoplasmic reticulum and many voltage-dependent channels[32].

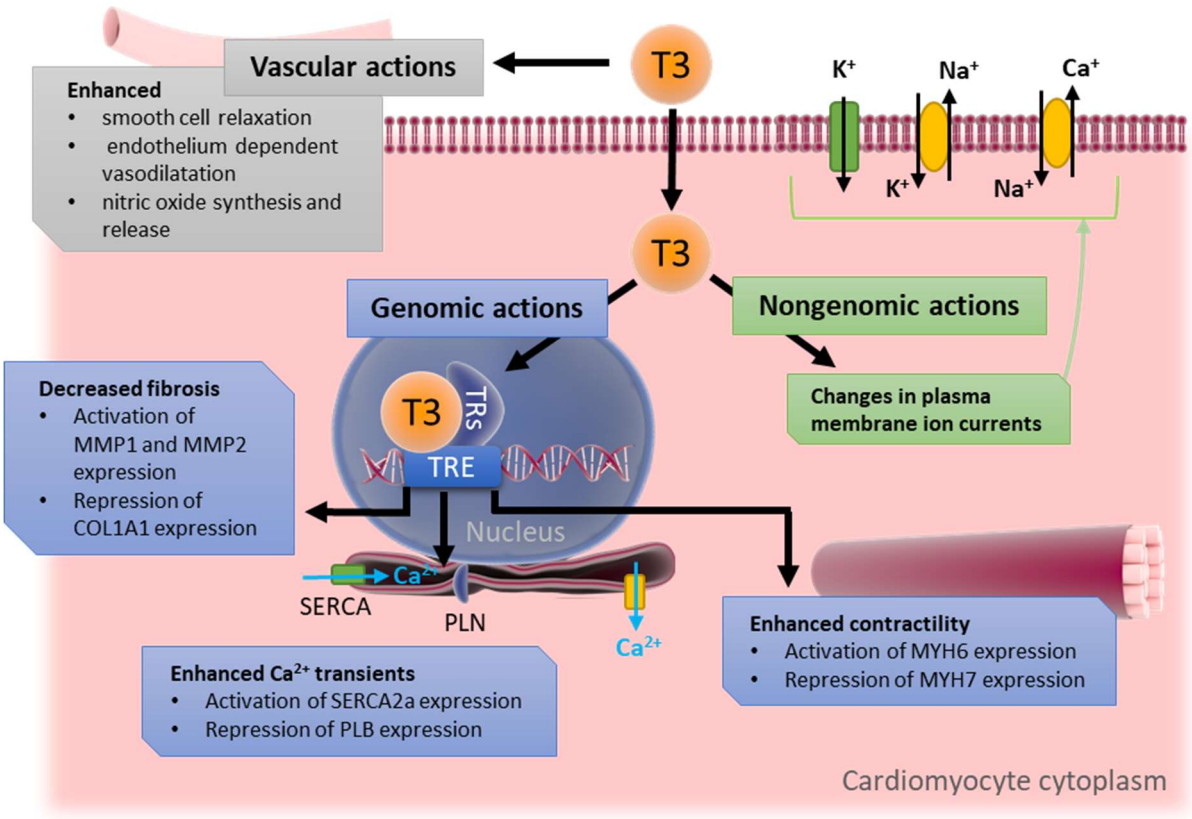

Figure 2: Effect of T3 on certain portions of the cardiovascular system via genomic and nongenomic actions. Binding of T3 (triiodothyronine) to thyroid hormone receptors (TRs) in the nucleus and subsequent interaction with thyroid hormone response elements (TRE) lead to the transcriptional regulation of diverse genes. Genes upregulated in this manner include MYH6 (myosin heavy chain-α), SERCA2a (sarcoplasmic/endoplasmic reticulum calcium ATPase 2 (SERCA2)) and MMP1/2 (matrix metalloproteinase-1/2). Downregulated genes include MYH7 (myosin heavy chain-β), PLB (phospholamban) and COL1A1 (collagen type I alpha 1 chain). Moreover, T3 modulates the activity of voltage-gated K^+ channels, Na^+/K^+ ATPase, and the Na^+/Ca^{2+} exchanger. T3 is also known to have considerable effects on the vascular system as a vasodilator. Adapted from Jabbar et al., (2016) [29].

Therefore, it comes as no surprise that various studies have described a correlation between overt hypothyroidism and both systolic and diastolic dysfunction in clinical and experimental context[32].

HF is known to be often accompanied by TH metabolism changes. A study reported that 22% of the HFpEF patients had reduced T3 levels[27]. These patients tended to be older, more

symptomatic, have hyperlipidemia, diabetes and higher levels of B-type natriuretic peptide (BNP)[27]. Small studies have also been able to find an inverse relationship between T3 levels and markers of HFpEF severity (via BNP, diastolic dysfunction and others)[27], but remained unable to answer an important question: is T3 dysfunction at the heart of HFpEF onset or is it just a consequence that further amplifies the problem?

Thyroid hormone dysfunction can take different forms, the most known being hypothyroidism and hyperthyroidism. Another more specific type of dysfunction, non-thyroidal illness, often referend to as low-T3 syndrome, has been reported in patients with cardiac disease[34] and is theorized to be an adaptive response mechanism to promote survival during cardiac disease[35]. In this syndrome, systemic fT3 and free thyroxine (fT4) levels are lowered, while thyroid stimulating hormone (TSH) is normal. This is the result of enzymatic conversion of T4/T3 to reverse T3 (rT3) - the inactive form – in peripheral tissues, while thyroid function is unaltered, hence the normal TSH levels. As it progresses and the severity increases, serum fT4 levels can also drop[36].

The mechanism behind thyroid hormones circulation, conversion and activity has already been extensively studied throughout the years[37]. The conversion of T4 and T3 to rT3 and T2, respectively, occurs via type 3 deiodinase (D3) (Figure 3). This enzyme's expression tends to be highly regulated but, under some pathological conditions, it has been shown to be overexpressed. One such example is HF, where it has been shown to be overexpressed in peripheral tissues but also in the heart[38]. Bearing this in mind and considering that serum THs

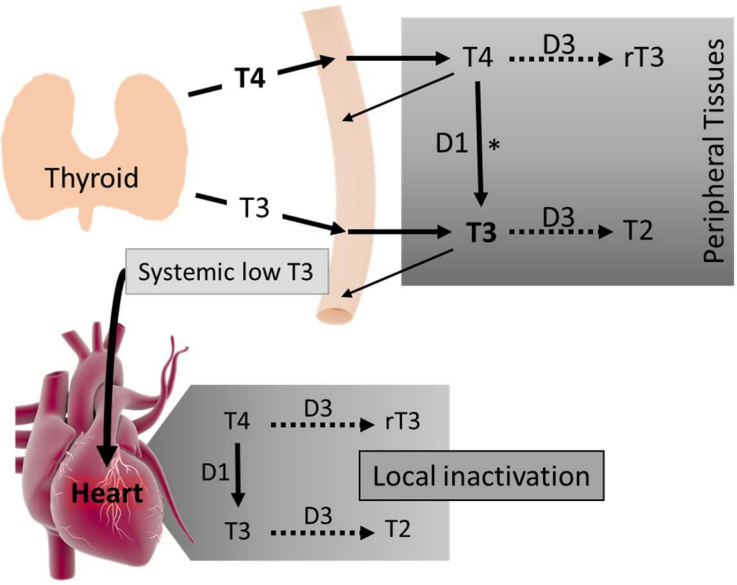

Figure 3: Metabolism of thyroid hormone in peripheral tissues, heart and central nervous system. In peripheral tissues ~40% of circulating T4 is converted to T3 by type 1 selenodeiodinase (D1). T3 is responsible for the majority of thyroid hormone action because it binds to the intracellular thyroid hormone receptor with 15-fold higher affinity than T4. The end result is altered gene expression in the target tissue. There are two subtypes of thyroid receptor (alpha & beta) expressed in different tissues, which contributes to differences in tissue sensitivity to thyroid hormone (Holt & Hanley, 2007). Propylthiouracil (PTU) inhibits the peripheral deiodination of T4 to T3.
* In the brain and pituitary T4 to T3 conversion is catalyzed by the Deiodinase 2 (D2) enzyme.
Adapted from Holt & Hanley, (2007) [38].

levels are already low due to peripheral degradation[39] it is reasonable to accept that THs levels can be further degraded in the heart, leading to even lower cardiac TH levels (Figure 3).

Considering all this data, an alarming relation seems to surface: HFpEF can lead to alterations in the thyroid axis, namely non-thyroidal illness, and local hypothyroidism, but concomitantly alterations in thyroid signalling can lead to further cardiac complications, in this case, progression of HFpEF[40–42]. This sort of positive-feedback loop can possibly be the source of worse prognosis in HF patients that present lower T3 levels at admission[30,43,44].

Currently, many questions concerning the relation between THs and HFpEF remains elusive. From the progression of TH alteration, its potential influence on the onset of the disease up to the mechanisms that lead to worse symptoms and prognosis of HFpEF. All of these knowledge gaps underlie the absence of a therapeutic strategy for HFpEF and emphasize the need for more research in this area.

As described earlier, HFpEF is a disease that, by nature and definition, imposes distinct functional alterations in the heart. These alterations are not circumscribed to cardiomyocytes but affect fibroblasts, extracellular matrix, endocardial vessels, translating to the whole heart function (Figure 2). Therefore, a lot of information can be obtained when dissecting and analyzing separately these components, such as the cardiomyocytes. This approach is particularly valuable since TH influence likely carries on, even after cardiomyocyte isolation, due to the *in vivo* chronic modulation of this axis.

Cardiomyocyte isolation has been first carried out over 40 years ago[45] and has, since, helped to understand the kinetic, molecular and physio-mechanic alterations present in the onset and progression of cardiac diseases[23,25,46–52]. Through the years, the availability of new technologies that allow researchers to simultaneously measure the Ca^{2+} transients and contractility of single cardiomyocytes added another layer of information extractable from this technique. One of these tools that warrants some further explaining is FURA-2. FURA-2 is a popular fluorescent dye used in the study of Ca^{2+} transients due to its inherent spectral properties and high affinity for free Ca^{2+}. Its fluorescence intensity increases directly with free

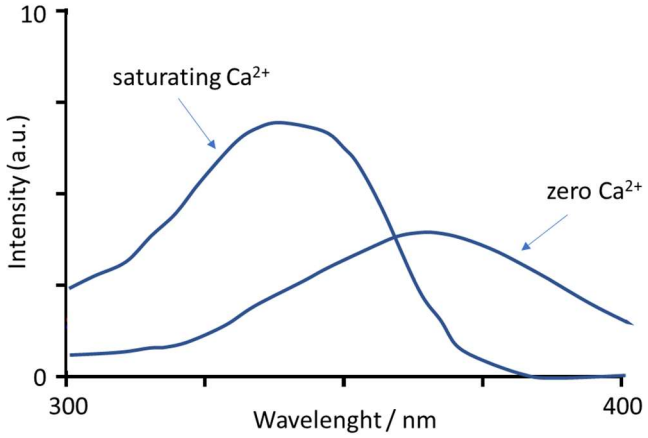

Figure 4: Excitation spectrum of 1 µM FURA-2, in a 20°C solution with pH 7.20, before and after the addition of saturating Ca^{2+} (2mM $CaCl_2$). Emission was collected at 500nm.

(Figure adapted from Grynkiewicz, G. et al., 1985). [41]

Ca^{2+} through 340nm excitation and in inversely proportional at 380nm (Figure 4), making it ideal for dual excitation ratio imaging. The ratio can therefore be used as an accurate

representation of free intracellular Ca^{2+} as it is the result of the emitted fluorescence of the bond and unbound species[53,54].

One technical struggle that researchers initially faced was the difficulty in loading cells with this fluorescent probe, since the dye is negatively charged it was unable to permeate the membrane without the need to disrupt it[53]. This changed with the addition of acetoxymethyl (AM) esters to FURA (FURA-2 AM), making it neutral and, thus, membrane permeable. Once inside the cell, esterases cleave off the AM esters by hydrolyzation leaving FURA trapped

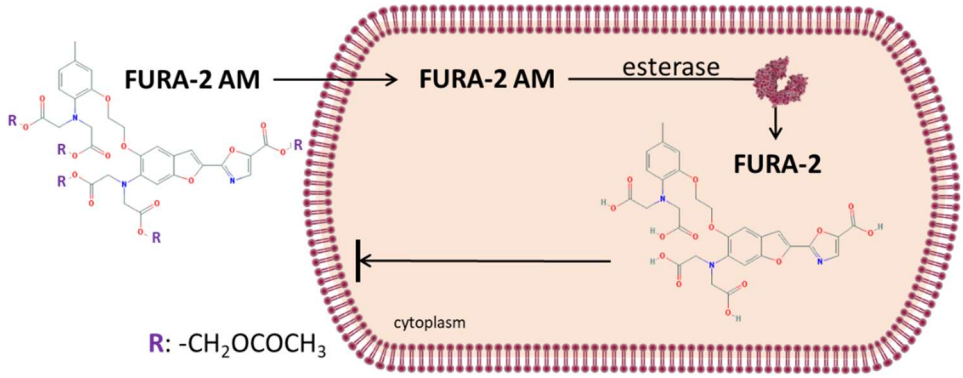

Figure 5: Cellular FURA-2 loading process. Example of a cell incubated with FURA-2 AM. This molecule can permeate the membrane and readily enters. Once inside, esterases hydrolyze the acetoxymethyl ends, leaving FURA-2 in its native form, unable to permeate and leave the cell.

inside the cell and available to bind to Ca^{2+}, making Ca^{2+} transient measurements possible (Figure 5).

With everything in mind and considering the impending need for a clinical answer to this disease, we hypothesize that preemptively targeting the thyroid axis in HFpEF patients might reveal to be a potent tool for the clinical practice if, among other comorbidities, a disruption in thyroid axis is found.

Chapter 2

Aims

The aim of the project is to assess if T3 administration can offer a safe therapeutic option for patients with high-risk of developing HFpEF presented with non-thyroidal illness or mild systemic hypothyroidism. To achieve this goal, we will characterize the impact of chronic modulation of systemic and local thyroid function (orally administered T3) in the metabolism and cardiac function of an animal model of HFpEF (obese ZSF1). Specifically, we will assess cardiac function on intact isolated cardiomyocyte's calcium (Ca^{2+}) and displacement transients. Moreover, we will correlate and integrate the results derived from this dissertation with preexisting data of the same animals, such as metabolic, echocardiographic, hemodynamic and morphometric data.

Chapter 3

Previous unpublished results

The Obese ZSF1 rat has been previously characterized by our group as a model of HFpEF [5]. At twenty weeks of age, the rats present lung congestion, preserved left ventricle (LV) systolic function, LV diastolic dysfunction, high filling pressures, cardiomyocyte stiffness and preserved renal function[10].

Here we outline some previous results that characterize the animals used in this study and present some functional data to further support some conclusions we reach in this dissertation. For this, the Obese ZSF1 rats (HFpEF) and Obese ZSF1 rat treated with T3 (HFpEF + T3) had their cardiac function evaluated at twenty-two weeks of age by echocardiography and at twenty-four weeks by invasive hemodynamics.

3.1 Thyroid hormone levels were significantly reduced in the left ventricle of HFpEF rats.

Frozen left ventricle sample were analyzed for local concentrations of T3 and T4 hormones to access the possibility of local hypothyroidism. Both hormones were found to be significantly reduced (Figure 6 A,B).

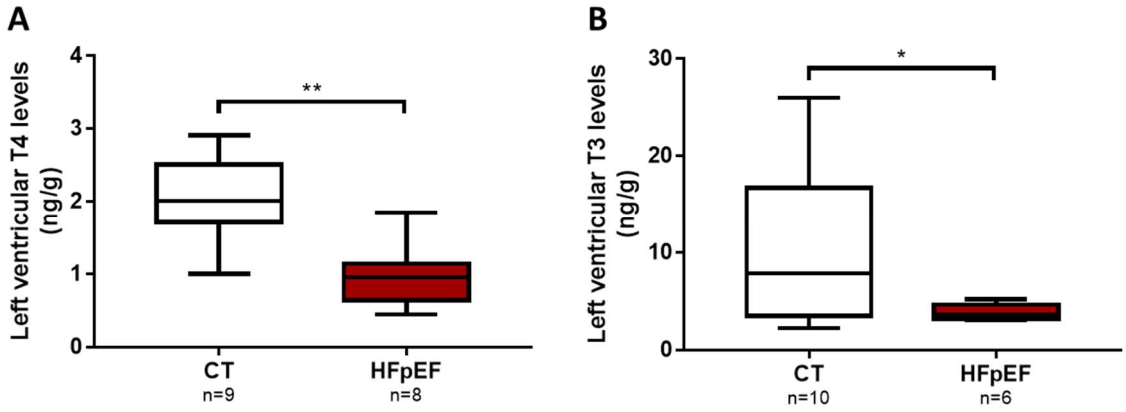

Figure 6: Left ventricular thyroid hormones levels. Left ventricular samples from ZSF1 Lean (CT) and ZSF1 Obese (HFpEF) rats were probed for their T4 **(A)** and T3 levels **(B)**. Error bars express the maximum and minimum value the parameter assumed. The middle line represents the median, while the box illustrates the first and third quartile. *: $p<0.05$ *vs* Lean; **: $p<0.01$ *vs* Lean.

3.2 T3 preemptive supplementation shows promising effects on morphometric, echocardiographic and hemodynamic analysis.

As previously described[1], HFpEF rats were obese, diabetic, as shown by worse oral glucose tolerance and increased insulin resistance, and presented heavier liver, subsequently confirmed as steatosis[55], compared to ZSF1 Lean (Table 2). Preventive T3 supplementation was found to significantly attenuate these parameters when compared to vehicle-treated rats.

Table 2 – Morphometric parameters

	CT (n=5)	HFpEF (n=8)	HFpEF + T3 (n=5)
Body Weight, g	451 ± 12	595 ± 21*	534 ± 18*#
Perigonadal fat, mg/cm²	640 ± 74	1617 ± 260*	1331 ± 66*
Perirenal fat, mg/cm²	732 ± 67	3857 ± 675*	2785 ± 255*#
OGTT AUC, mg/min/dl	12009 ± 219	36949 ± 2067*	24056 ± 1561*#
IR AUC, mg/min/dl	6777 ± 511	16125 ± 1014*	11292 ± 169*#
Liver Weight, mg/cm²	3047 ± 147	10253 ± 478*	7035 ± 806*#

Insulin resistant tests conducted at week 18 and glucose tolerance at week 22. OGTT, oral glucose tolerance test; AUC, area under curve; IR insulin resistance. Values are mean ± SEM.
*: $p<0.05$ *vs* CT; #: $p<0.05$ *vs* HFpEF.

Measurements of arterial pressure revealed that, unlike both systolic and mean, diastolic arterial pressure shown a tendency to ameliorate with the therapy (100 ± 4 *vs* 85 ± 5, $p=0.06$). Accordingly, a significant rise in pulse pressure was also registered (51 ± 2 *vs* 64 ± 4, $p<0.05$).

Echocardiographic studies (Table 3) revealed that HFpEF rats had an increase of left ventricle mass, denoting left ventricle hypertrophy, and a reduction of IVRT, E/e' and LAA, reflecting abnormalities in left ventricle relaxation and filling. T3 treatment was found to be effective at attenuating these changes, thus effectively ameliorating diastolic function.

Moreover, T3 supplementation was also found to enhance systolic function, detected by normalization of S'.

Hemodynamic studies of HFpEF rats found a significantly decrease of heart rate without alterations in ejection fraction, however neither cardiac index nor ejection fraction were significantly reduced, denoting the preservation of systolic function (Table 4). Myocardial relaxation was impaired since exponential Tau (Texp) was increased. The increased left ventricle stiffness was evidenced by the augment of chamber stiffness constant β and by the trend of end-diastolic pressure to increase in HFpEF rats compared to CT. Likewise, arterial elastance was also higher in HFpEF rats.

Table 3 – Echocardiographic data at 22 weeks of age

	CT (n=5)	HFpEF (n=8)	HFpEF + T3 (n=5)
LV mass (g)	1.11 ± 0.17	1.52 ± 0.04*	1.49 ± 0.08*
IVCT (ms)	16.29 ± 1.55	15.63 ± 0.61	14.00 ± 0.74
IVRT (ms)	20.67 ± 1.44	24.45 ± 0.68*	20.47 ± 1.18#
ET (ms)	73.25 ± 2.00	83.64 ± 2.47*	65.07 ± 2.06*###
S' (m/s)	0.066 ± 0.003	0.046 ± 0.002*	0.063 ± 0.005##
E/e'	15.03 ± 2.35	21.05 ± 1.12*	16.20 ± 1.09#
E/A	1.97 ± 0.34	1.61 ± 0.12	1.80 ± 0.17
LAA (cm^2)	0.28 ± 0.01	0.36 ± 0.01***	0.32 ± 0.01#

LV, left ventricle; IVCT, isovolumetric contraction time; IVRT, isovolumetric relaxation time. ET, ejection time; S', peak systolic velocity of tissue Doppler at the lateral mitral annulus; E/A, ratio between peak E and A waves of pulsed-wave Doppler mitral flow velocity; E/E', ratio between peak E wave velocity of pulsed-wave Doppler mitral flow and peak E' wave velocity of tissue Doppler at the lateral mitral annulus; LAA, left atrial area. Values are mean ± SEM. *: p<0.05 vs Lean; ***: p<0.001 vs Lean #: p<0.05 vs HFpEF, ##: p<0.01 vs HFpEF, ###: p<0.001 vs HFpEF.

Table 4 – Hemodynamics data at 24 weeks of age

	Lean (n=5)	HFpEF (n=8)	HFpEF + T3 (n=5)
BSA, $g.cm^{-2}$	535 ± 9	672 ± 4*	629 ± 8*#
CI, $\mu l.min^{-1}.cm^{-2}$	140 ± 9	127 ± 6	158 ± 10#
HR, min^{-1}	340 ± 13	282 ± 12*	314 ± 16
EF, %	60 ± 1	63 ± 3	77 ± 6*#
T_{exp}, ms	10.7 ± 0.5	12.7 ± 0.4*	8.6 ± 0.7*#
EDP, mmHg	8.0 ± 1.2	12.1 ± 1.4	9.7 ± 1.0
EDV_i, $\mu l.cm^{-2}$	0.72 ± 0.03	0.74 ± 0.05	0.68 ± 0.05
Ea_i, $mmHg.\mu l^{-1}.cm^{-2}$	536 ± 9	673 ± 4*	629 ± 8*#
β, $\mu l.cm^{-2}$	4.68 ± 0.72	7.94 ± 0.91*	5.93 ± 0.53
E_{esi}, $mmHg.\mu l^{-1}.cm^{-2}$	161 ± 17	196 ± 18	242 ± 36

BSA, body surface area; CI, cardiac index; HR, heart rate; EF, ejection fraction; T_{exp}, time constant of isovolumetric; EDP, end-diastolic pressure; EDV, End-diastolic volume; Ea, arterial elastance; β chamber stiffness constant derived from exponential; EDPVR; E_{ES}, slope of linear end-systolic pressure–volume relationship. Values are mean ± SEM. *: p<0.05 vs Lean; #: p<0.05 vs HFpEF.

Meanwhile, T3 treated rats showed clear evidence of heart function amelioration, namely an increase of cardiac index and ejection fraction, as well as a reduction of relaxation time and arterial elastance. These rats also displayed a trend towards reduced end-diastolic pressures and chamber stiffness constant β.

Together these results show that T3 had a clear positive impact on systolic, diastolic and vascular function.

Chapter 4

Methods and Materials

4.1 Animal model and experimental protocol

All animal experiments were approved by the ethics committee of the Faculty of Medicine of University of Porto and by the Portuguese Direção-Geral de Alimentação e Veterinária (DGAV) and performed according to the Guide for the Care and Use of Laboratory Animals published by the NIH (NIH Publication no. 85–23, revised 2011). The Faculty of Medicine of University of Porto is a governmental institution, granted approval by the Portuguese government to perform animal experiments.

Twelve-weeks old age-matched male ZSF1 lean (CT, n=5) and Ob (HFpEF, n=16) were obtained from Charles River (Barcelona, Spain) and housed in groups of two animals per cage in an isolated ventilated cage system (IVC), maintained on a 12-hour light-dark cycle, with full access to the recommended diet (LabDiet® 5008, International Product Supplies Ltd.) and water *ad libitum*. The IVCs were maintained under controlled environment temperature (22°C), relative humidity (30–70%), and air exchange rate (40–50 air changes per hour).

As depicted in Figure 7, by thirteen weeks of age, a subgroup of ZSF1 obese rats (HFpEF+T3, n=8) was randomly allocated to receive T3 (0.04/0.06 µg/ml, T6397, Sigma) supplementation in drinking water. Dosage was calculated by titration over the protocol in order to obtain blood free T3 (fT3) levels analogous to the CT group, with an initial T3 concentration in the water of 0.04 µg/ml, increased to 0.06 µg/ml after 4 weeks. Weight gain and energy intake were recorded every second day. Phenotypic evaluation was repeated at the 14^{th}, 18^{th} and 22^{th}. Starting at this time-point, animals underwent several evaluations till twenty-two weeks of age: serial serum TH assessment (TSH, fT3 and fT4 using ELISA methods), metabolic cage studies, insulin resistance (IR) and oral glucose tolerance testing, effort testing with maximum O_2 consumption (VO_2max - closed chamber treadmill at 15° inclination coupled to a gas analyzer) determination and echocardiographic evaluation for cardiac characterization. Briefly, anesthetized rats were placed on a heating pad and the ECG was monitored. A linear 15 MHz probe (Sequoia 15L8W) was used and parasternal short axis view was performed to record M-mode as previously described[5]. Aortic and mitral flow tracing velocity were recorded by pulsed-wave Doppler. Peak systolic tissue velocity and E' were measured with tissue Doppler at the medial mitral annulus. Maximal left atrial dimensions were measured

by 2D echocardiography in the four-chamber view. Acquisitions were done while transiently suspending mechanical ventilation and recordings from three consecutive heartbeats were averaged.

From twenty-two to twenty-four weeks of age, animals undergone a terminal hemodynamic evaluation. Summarily, anaesthetized rats were endotracheally intubated, mechanically ventilated. After femoral vein cannulation and lateral thoracotomy, pericardium was widely opened and a pressure–volume catheter was implanted through the apex along the LV and a perivascular flow probe placed around the aorta to measured cardiac output. The signals were continuously acquired baseline and after vena cava or aortic occlusions as previously described[56].

At the end, the animals were euthanized under anesthesia by exsanguination. Once concluded, the heart was removed, and the apex was quickly cut and frozen for biochemical and molecular studies. The remaining heart was swiftly used for cardiomyocyte isolation. The lungs, liver, perirenal and perigonadal fat were weighed, snap frozen in liquid nitrogen and stored at −80°C. The weights were normalized to tibia length given the body weight differences observed between groups. Extended details of these procedures are presented in appendix.

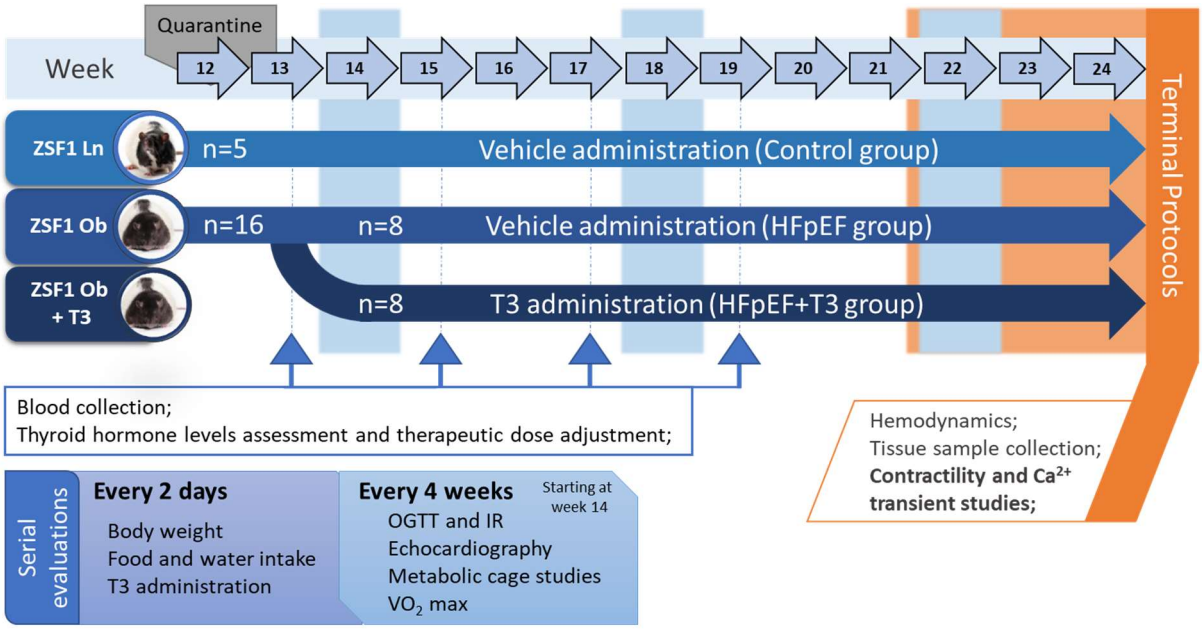

Figure 7: Animal study design for the experimental protocol. At arrival, animals were held in quarantine and allowed to adapt. At the age of 13 weeks ZSF1 Ob rats were randomly allocated to receive T3 in the drinking water or simply water. Animals were followed daily and assessments were conducted every 2 and 4 weeks. Terminal protocols started at week 22 and lasted till week 24.
OGTT, Oral glucose tolerance test; IR, Insulin resistance.

4.2 Thyroid function assessment by ELISA

Blood samples collected from subclavian vein after echocardiographic evaluation were placed in tubes with EDTA. Samples were centrifuged at 5000 rpm for 15 minutes at 4°C, plasma or serum was then separated and utilized for quantitative enzyme immunoassays (ELISA). fT3

(1225-300, AccuBind), fT4 (1325-300, AccuBind) and fTSH (55-TSHRT-E01, ALPCO) ELISA kits were used to determine the levels of the corresponding serum hormone according to the manufacturer's instructions. Results were analyzed using an ELISA plate reader (UVM-340, ASYS Hitech GmbH, Austria) and a calibration curve was constructed by plotting the absorbance values at 450nm (with specific correction, according to manufacturer's protocol) and concentrations of unknown samples were determined.

4.3 Cardiomyocyte Isolation

The heart was cannulated via the aorta and perfused at 6mL/min with cold Ca^{2+}-free digestion buffer (DB) (in mM: 130.00 NaCl, 5.40 KCl, 3.00 Pyruvate, 25.00 HEPES, 0.50 $MgCl_2 \cdot 6H_20$, 0.33 $NaH_2PO_4 \cdot H_20$ and 22.00 Glucose) supplemented with 0.05mM HEPES and 0.2mM EGTA as quickly as possible. Care was given throughout the whole protocol to avoid any bubble from entering the perfusion system as it drastically affects the isolation.

Once the drips were clear (no visible blood denoting that coronary arteries are cleaned), perfusate was changed to solution 1 (Table 5) at 37°C. Enzyme digestion duration can depend on several factors, so it can vary significantly between animals (35-55 minutes in our experiment). A good visual indicator that this step is complete is the progressive 'whitening' of the heart and soft to the touch.

After transferring the heart to solution 2 (Table 5) at 37°C, the tissue was thoroughly minced and mechanical trituration for 3 minutes, the solution was then strained through a 200µm mesh and centrifuged at 500 rpm for 1 min, at room temperature. The pelleted cells were resuspended in solution 3 (Table 5) and left to precipitate for 10 minutes at room temperature. The solution cells were then resuspended in solution 4 (Table 5) for another 10 minutes.

Finally, the supernatant was removed and exchanged by Tyrode's buffer (in mM: 133.5 NaCl, 5.0 KCl, 1.2 $NaH_2PO_4 \cdot H_20$, 1.2 $MgSO_4$, 10.0 HEPES and 22.0 Glucose) with 1.8mM Ca^{2+}.

All solutions used in this protocol had a physiologic controlled pH of 7.40 at 37°C. The glassware and instruments are sterilized by autoclaving at 121°C or by procedures recommended by the manufacturer.

Table 5 – Digestion solutions used in the isolation procedure

Solution in digestion buffer	1	2	3	4
Collagenase type 2 (17101, Gibco), mg/mL	1.2	0.3	-	-
$CaCl_2$, mM	0.05	0.1	0.25	0.5
Bovine Serum Albumin (MB04602), mg/mL	-	10	10	10

4.4 Calcium transient and sarcomere and sarcomere shortening recording

Cardiomyocyte were placed in temperature-controlled MatTek dishes at 37^{o}C, containing 1.8mM Ca^{2+} Tyrode's buffer. Platinum electrodes were immersed in the solution for stimulation, coupled to a MyoPacer (IonOptix, Milton, USA). Ca^{2+} transients and sarcomere were simultaneously recorded in an inverted microscope by an IonOptix system (IonOptix, Milton, USA) similarly to what has been previously described[57–60]. Briefly, cardiomyocytes were placed in a heated chamber mounted on the stage of an Olympus AE31 inverted microscope. After selection of an isolated, rod-shaped cardiomyocyte that was optically intact, presented clear striation and did not spontaneously contract, the analysis was initiated.

Prior to measuring, the solution containing the intact isolated cardiomyocytes was incubated for 20 min with a Ca^{2+} sensitive dye, 1mM FURA-2AM (ThermoFisher, F1221). After changing the FURA-2AM for fresh Tyrode's buffer and repeating this washing step after 5 minutes, the cells were loaded and ready to measure 20 mins after.

Loaded cells were electrically stimulated (IonOptix MyoPacer, Milton, USA) at different frequencies with 14 ms bipolar pulse waves. Frequencies were changes every minute from the begging of the measurement as follows: 1Hz -> 0.5Hz -> 1Hz -> 2Hz -> 4Hz. The fluorescence emitted at 340 nm and 380 nm was alternately recorded and a ratiometric fluorescence/fluorescence ratio was made as an indicator of cytosolic Ca^{2+} concentration. At the same time, light filtered with a filter permissive only to red light in the visible spectrum (650-750 nm) illuminated the cell in study thought the bright-field path of the microscope.

Sarcomere shortening was recorded by making use of the inherent very regular organization of the sarcomere for optical detection. The transverse pattern that emerges from the thin actin (light) filaments and thick (dark) filaments of myosin can be adjusted to a sinusoidal curve by a Fourier spectrum analysis[61]. The distance sarcomere length can then be derived from the distance between bands of myosin, obtained from the frequency of the sinusoid curve. Live recordings entail the constant computing and recording of the spatial frequency for each frame of the user selected region.

All steps above were carried out in a dark room, with special care to avoid any and all light-exposure. Acquired raw data was analyzed using IonWizard 6.6.4.112 software (IonOptix, Milton, USA).

4.5 Data and Statistical Analysis

Echocardiographic and hemodynamic statistical analysis was performed using GraphPad Prism (version 7.0, GraphPad Software, Inc.). Analysis by one-way ANOVA was used for comparison among groups. When treatments were significantly different, the Holm-Sidak test and Bonferroni test was selected to perform pairwise comparisons. Group data are presented as mean ± SEM.

Data obtained from isolated cardiomyocyte measurements using the IonOptix system was analyzed using the bundled proprietary software IonWizard (6.6.4.112, IonOptix LLC). Fluorescence data from each individual cardiomyocyte was subjected to background subtraction. The data analyzed, sorted by stimulation frequency and several different parameter values were evaluated.

Previous to statistical analysis, data was run through an outlier detection. This is not essential, but highly recommended given the nature of the biological material and basis of this technique. Even the most robust animal model is prone to variability. That is why several cells were analyzed per animal, however, sometimes erratic cells end up being recorded, but thanks to the high reproducibility of this technique it is easy to detect these outliers. For this end, a ROUT identification with Q = 1 % was conducted (version 7.00, GraphPad Software, Inc.).

Each parameter was analyzed via column statistics to check for normal distribution using the D'Agostino-Pearson omnibus normality test. When a set of data did not pass the normality test, a Kruskal-Wallis test (non-parametric test) was conducted. In the case that normal distribution of data was confirmed, a regular one-way ANOVA was used. Statistical analysis was conducted used GraphPad Prism (version 7.00, GraphPad Software, Inc.). The level of significance was set at $p < 0.05$.

Chapter 5

Results

As mentioned before, this dissertation is a part of a major project that intends to characterize the TH axis alterations in progression towards HFpEF and to determine if T3 modulation might be a valid therapeutic option at the onset of the disease. For this, multiple methodologies were used, but herein we will focus on the measurement of Ca^{2+} transients and sarcomere shortening as these can give us an excellent and unique understanding of cardiomyocyte function and remodeling, as well as, serve to corroborate, at the cell level, findings derived from other techniques, such as hemodynamics and echocardiography.

5.1 T3 levels are lowered in the HFpEF (Obese ZSF1) compared to control rats (Lean ZSF1). T3 supplementation did not normalize T3 levels.

Serum fT3 hormone levels strongly tended to be reduced in both HFpEF groups when compared to the CT throughout the whole experience (Figure 8.A). At the start of the experiment, fT4 is also decreased in the HFpEF groups compared to CT. Meanwhile, two weeks after the start of the supplementation, fT4 levels fell in the T3 treated group and remained the lowest throughout the weeks (Figure 8.B). Lastly, serum free TSH levels were similar across all groups (Figure 8.C).

Of note, the mortality rate was absent in both CT and vehicle-treated HFpEF rats, but T3 treatment resulted in the unforeseeable death of three animals, one with 17 week of age and the other two with 23.

5.2 HFpEF rats showed delays in Ca^{2+} transients in both contraction and relaxation and T3 supplementation significantly reverts this delay

Electrical stimulation of intact cardiomyocytes allowed to plot cytoplasmic Ca^{2+} transients as a fluorescence ratio between 340 and 380nm (Figure 9.A). Upon 1 Hz stimulation, Ca^{2+} transients were found to be delayed in HFpEF rats both in the contraction, as assessed by the time to peak Ca^{2+} (Figure 9.B) and in the relaxation, as measured in half-time of peak Ca^{2+} decay (Figure 9.C).

Interestingly, T3 supplementation (HFpEF + T3) seemed to revert this delay, both in contraction (Figure 9.B) and relaxation (Figure 9.C) to CT levels.

Lastly, Ca^{2+} transient amplitudes were conserved across the experimental groups, but a slight trend towards lower amplitudes was detected in the treated group (Figure 10.D).

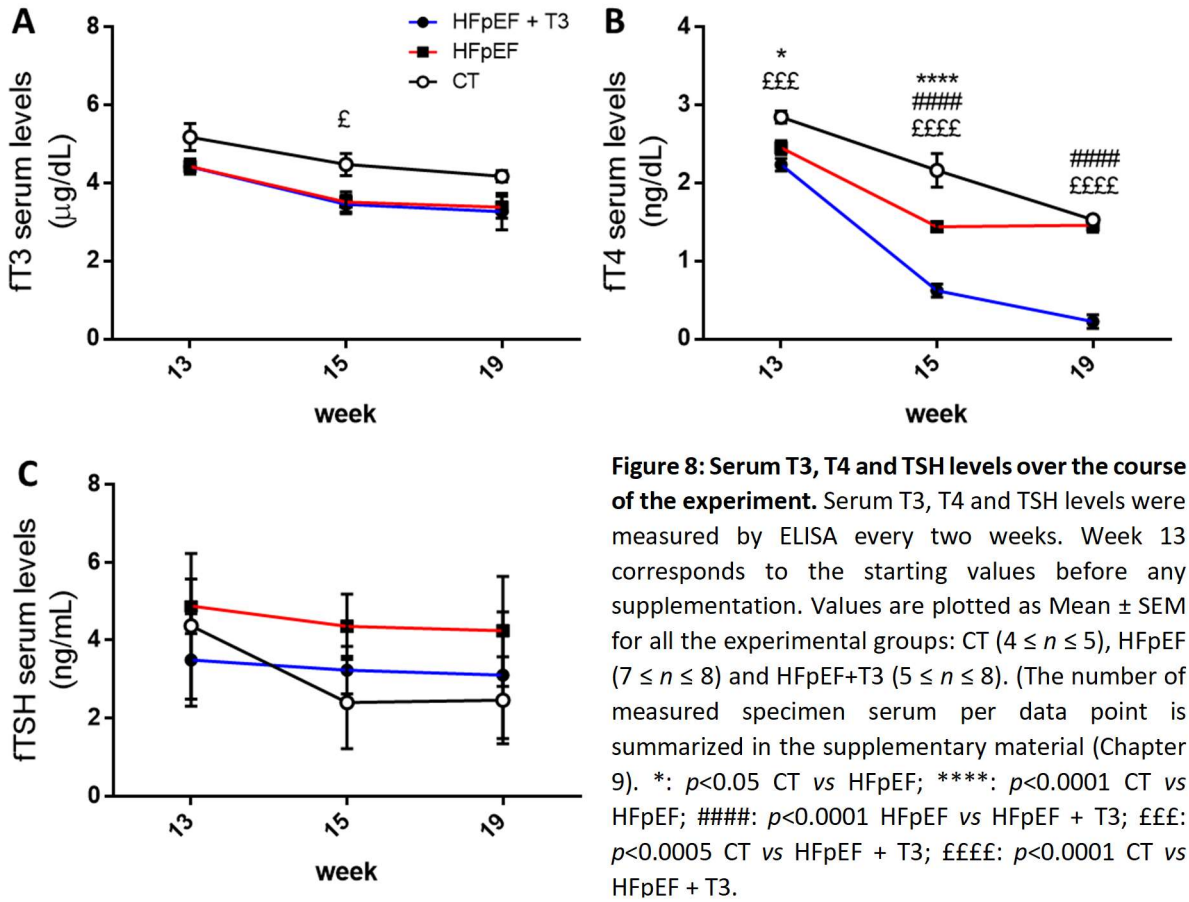

Figure 8: Serum T3, T4 and TSH levels over the course of the experiment. Serum T3, T4 and TSH levels were measured by ELISA every two weeks. Week 13 corresponds to the starting values before any supplementation. Values are plotted as Mean ± SEM for all the experimental groups: CT ($4 \leq n \leq 5$), HFpEF ($7 \leq n \leq 8$) and HFpEF+T3 ($5 \leq n \leq 8$). (The number of measured specimen serum per data point is summarized in the supplementary material (Chapter 9). *: $p<0.05$ CT *vs* HFpEF; ****: $p<0.0001$ CT *vs* HFpEF; ####: $p<0.0001$ HFpEF *vs* HFpEF + T3; £££: $p<0.0005$ CT *vs* HFpEF + T3; ££££: $p<0.0001$ CT *vs* HFpEF + T3.

5.3 T3 supplementation prevents HFpEF induced delay in sarcomere contractility

Cardiomyocytes require Ca^{2+} influxes to the cytoplasm to develop force and contract, therefore, a delay in Ca^{2+} transients will be reflected on contraction delays.

Our data corroborates this, displaying different contractile profiles under pacing depending on the experimental group (Figure 10.A). As expected, HFpEF was associated to a longer time to reach full contraction, whereas T3 not only reverted this delay, but significantly decreased it in comparison with CT (Figure 10.B).

Cardiomyocytes isolated from HFpEF took the longest to reach a state of half-relaxation (Figure 10.C), while those extracted from T3 treated rats displayed a significant shorter time to half-relaxation when compared to both HFpEF and CT.

Shortening analysis using single exponential Tau provides further insight into the relaxation period, revealing that HFpEF takes indeed longer than CT to relax (Figure 10.D) providing further evidences of impaired relaxation. Additionally, this indicates that while T3 took

significantly less time to reach a state of half-relaxation, in the end, both CT and T3 treated cells shared similar relaxation speed.

Sarcomere amplitude at the peak of contraction was found to be significantly impaired in HFpEF, whereas T3 treated cardiomyocytes presented similar contraction amplitude capabilities as those from CT rats (Figure 10.E).

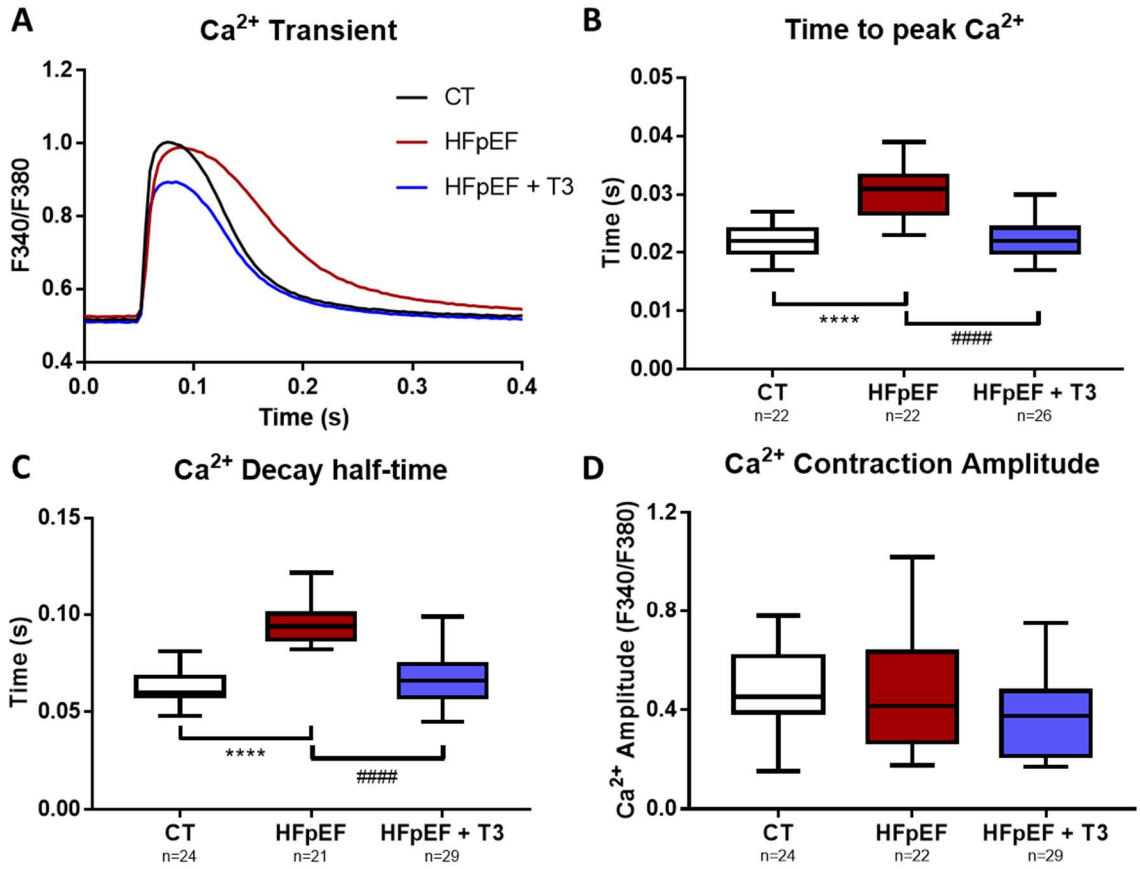

Figure 9: Ca^{2+} measurements. (A) Average Ca^{2+} transient fluorescence ratio plotting recording with 1 Hz electrical stimulation frequency for the different experimental groups: CT (ZSF1 Lean, n=24), HFpEF (ZSF1 Obese, n=22) and HFpEF + T3 (ZSF1 Obese + T3, n=29). (B) Time elapsed from electric stimulus until peak cytoplasmic Ca^{2+} level was attained. (C) Time interval from peak Ca^{2+} to its half decay (50 % of peak Ca^{2+}). **(D)** Contraction amplitude, measured by subtracting the peak FURA-2 fluorescence ratio (F340/380) by the baseline, for each experimental group: CT (ZSF1 Lean), HFpEF (ZSF1 Obese) and HFpEF + T3 (ZSF1 Obese + T3). Error bars express the maximum and minimum value the parameter assumed. The middle line represents the median, while the box illustrates the first and third quartile.
****: p<0.0001 CT *vs* HFpEF; ####: p<0.0001 HFpEF *vs* HFpEF + T3.

5.4 T3 treatment significantly reduces contraction cycles

The time duration from half the contraction to half the relaxation can provide a good measure of contraction and relaxation response. In this regard, HFpEF contractility cycle seems to be compromised while T3 treatment significantly reduces the contraction time, even compared to the CT group (Figure 10.F).

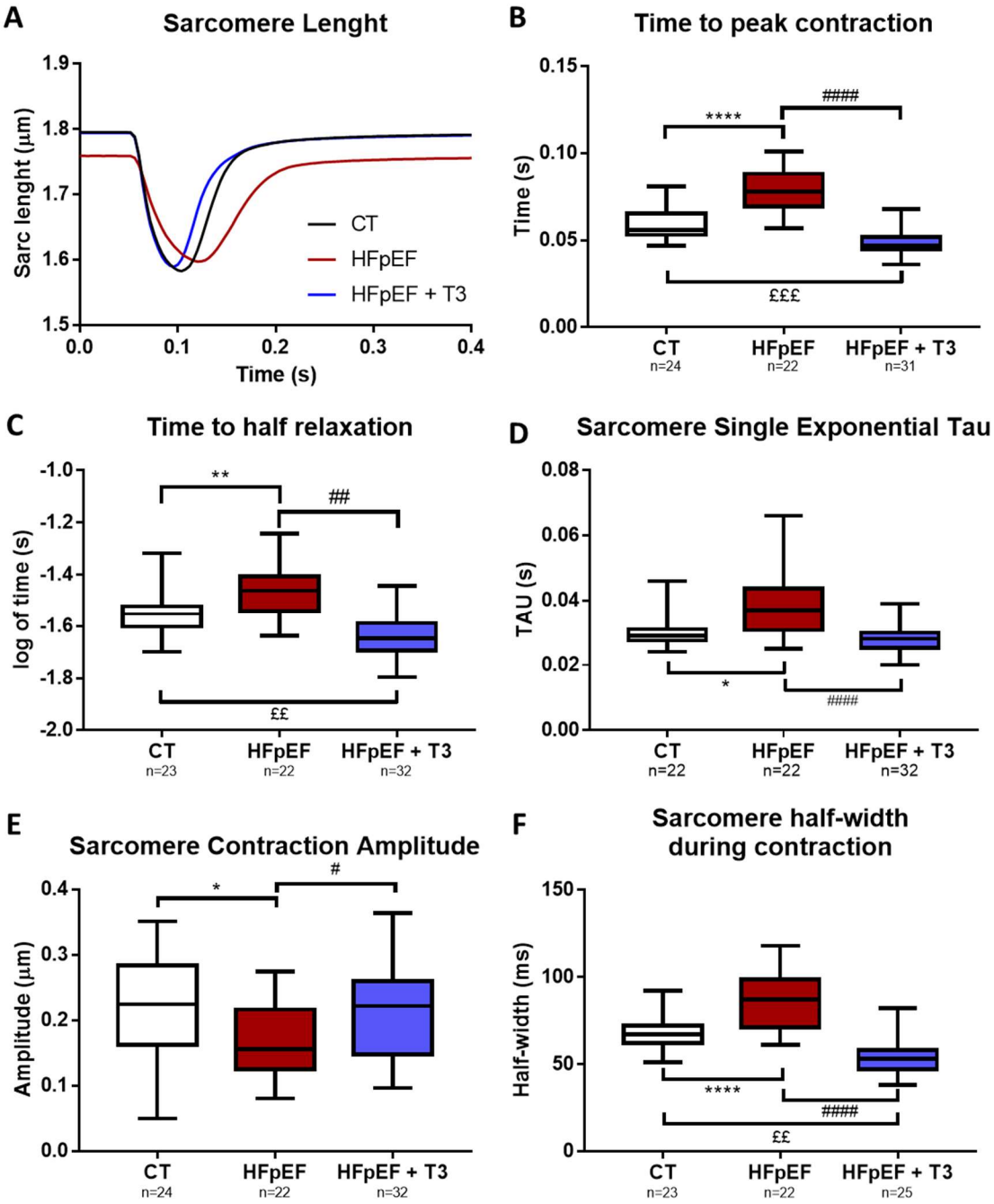

Figure 10: Contraction measurements. (A) Average sarcomere length recording with 1 Hz electrical stimulation frequency for the different experimental groups: CT (ZSF1 Lean, n=24), HFpEF (ZSF1 Obese, n=22) and HFpEF + T3 (ZSF1 Obese + T3, n=32). **(B)** Time elapsed from electric stimulus to when peak sarcomere shortening was attained. **(C)** Time interval from peak sarcomere shortening to a half-relaxed state. **(D)** Sarcomere single exponential Tau is used to characterize the speed of recovery, in this case, the speed of relaxation till the baseline (relaxed state). This analysis was performed for each experimental group: CT (ZSF1 Lean), HFpEF (ZSF1 Obese) and HFpEF + T3 (ZSF1 Obese + T3). **(E)** Sarcomere contraction amplitude upon stimulation. Error bars express the maximum and minimum value the parameter assumed. **(F)** Sarcomere contraction half-with as measured by the time interval between a half- contraction and half-relaxation state. Error bars express the maximum and minimum value the parameter assumed. The middle line represents the median, while the box illustrates the first and third quartile.

*: $p<0.05$ CT *vs* HFpEF; ****: $p<0.0001$ CT *vs* HFpEF; #: $p=0.0346$ HFpEF *vs* HFpEF+T3; ####: $p<0.0001$ HFpEF *vs* HFpEF+T3; ££: $p<0.01$, £££: $p=0.0003$ CT *vs* HFpEF+T3.

5.5 The shorter resting sarcomere length of HFpEF was corrected by T3 administration

Measurements of the resting sarcomere length (without electrical pacing) revealed that HFpEF rat cardiomyocytes had shorter basal sarcomere length. This was already hinted at by careful analysis of Figure 11 and is quantitatively displayed in Figure 12.

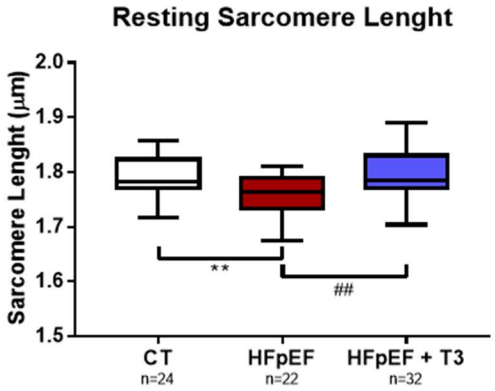

Figure 11: Basal sarcomere length measured in the lack of electrical stimulation for each experimental group: CT (ZSF1 Lean), HFpEF (ZSF1 Obese) and HFpEF + T3 (ZSF1 Obese + T3). Error bars express the maximum and minimum value the parameter assumed. The middle line represents the median, while the box illustrates the first and third quartile.
**: *p*=0.0085 CT *vs* HFpEF; ##: *p*=0.008 HFpEF *vs* HFpEF+T3;

5.6 T3 prevents the Ca^{2+} accumulation in the cytoplasm observed in HFpEF cardiomyocytes at higher pacing frequencies

When paced at 1 Hz (Figure 9) cardiomyocytes, regardless of the experimental group, all shared the same fluorescence baseline. Interestingly, when at 4 Hz (Figure 12.A) a rise in the baseline is evidenced. This rise, quantitatively illustrated in Figure 12.B, was not accompanied by an increase in the fluorescence amplitude at the time of peak contraction (Figure 12.C).

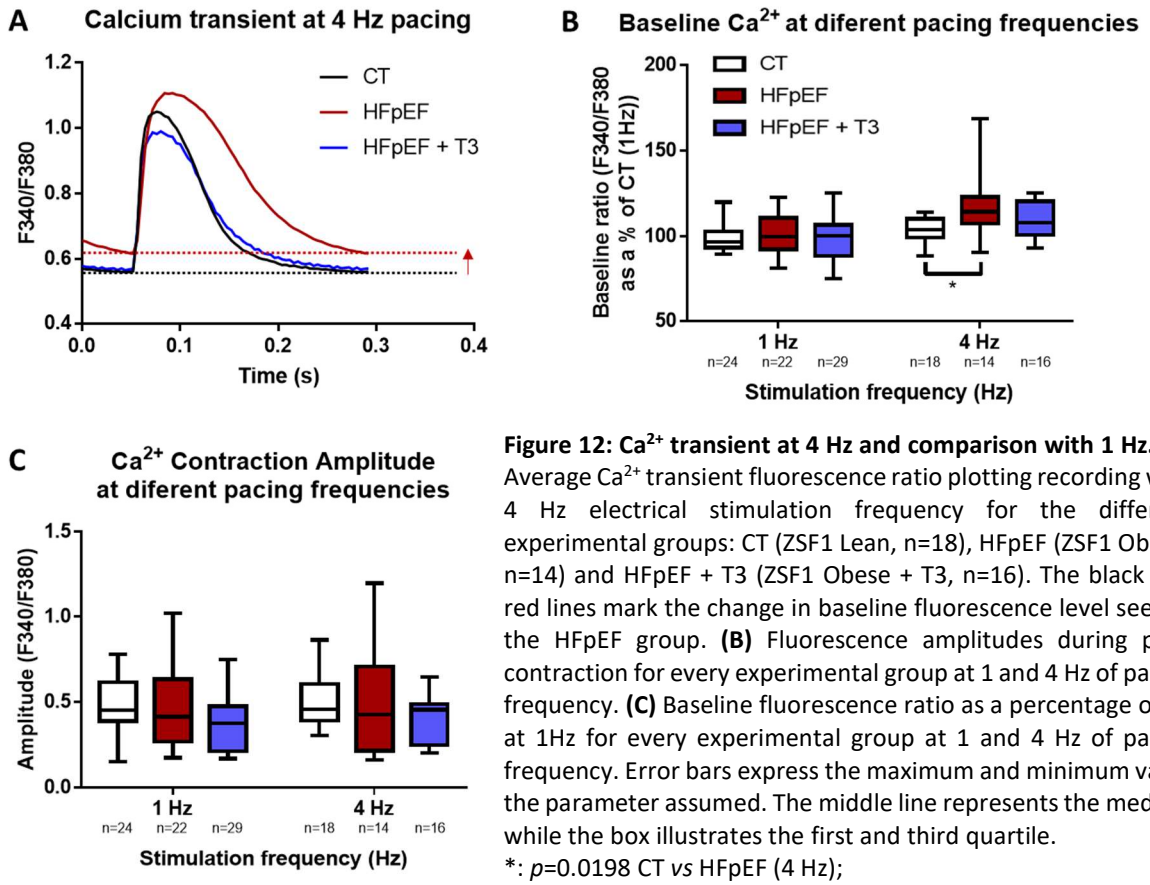

Figure 12: Ca^{2+} transient at 4 Hz and comparison with 1 Hz. (A) Average Ca^{2+} transient fluorescence ratio plotting recording with 4 Hz electrical stimulation frequency for the different experimental groups: CT (ZSF1 Lean, n=18), HFpEF (ZSF1 Obese, n=14) and HFpEF + T3 (ZSF1 Obese + T3, n=16). The black and red lines mark the change in baseline fluorescence level seen in the HFpEF group. **(B)** Fluorescence amplitudes during peak contraction for every experimental group at 1 and 4 Hz of pacing frequency. **(C)** Baseline fluorescence ratio as a percentage of CT at 1Hz for every experimental group at 1 and 4 Hz of pacing frequency. Error bars express the maximum and minimum value the parameter assumed. The middle line represents the median, while the box illustrates the first and third quartile.
*: *p*=0.0198 CT *vs* HFpEF (4 Hz);

Chapter 6

Discussion

This project seeks to explore the underlying functional alterations that are at the basis of HFpEF and shed some light on the potential functional benefits of long term T3 supplementation as an effective therapy for HFpEF. Herein we focus solely on the cardiomyocyte functional alterations and, to do so, we started by implemented a new technique that allowed us to study contraction and Ca^{2+} handling.

The main results from this study are: (1) Cardiomyocytes isolated from HFpEF rats (ZSF1 Obese) shown impaired Ca^{2+} transients patent in both contraction and relaxation; (2) Sarcomere contraction cycle was also found to be delayed in HFpEF cardiomyocytes; (3) T3 treated HFpEF rats (ZSF1 Obese + T3) displayed significant recovery, albeit the quickened sarcomere contraction and initial relaxation when compared to control and (4) The results obtained in isolated cardiomyocytes in vitro are in agreement with the in vivo results of each group, highlighting that the functional alterations observed in the heart are mostly derived from cardiomyocytes changes.

In particle physics the vast majority of data is obtained by looking at the building blocks of atoms, after all studying the parts that lead up to the whole is essential. This seems to be ubiquitous to numerous fields of study such as the pathophysiological mechanisms of cardiac diseases. Accordingly, to study cardiac pathology, we should, analyze all components of the heart individually and combined as a whole. With this in mind, in this dissertation, we started by focusing on cardiomyocytes, given their importance in determining ventricular function and since they constitute the principal source of mass in the heart, even though they do not represent the majority of cells in the heart[62].

The first report of successful isolation of viable cardiomyocytes dates back to 1955[63] and has, ever since, opened the possibility to several techniques. Some of these techniques, can provide important functional data that is unique to single cell studies and fully complement other studies. A practical example of this applied to the present study is the data we obtained from the echocardiography, as it did not allow us to distinguish with reasonable certainty if the source of functional alterations we identified lied in cardiac impairment, vascular dysfunction or a mix of both. By directly studying isolated cardiomyocytes, we were able to evaluate several parameters that have direct correlations to cardiac (patho)physiology.

6.1 Animal model

As mentioned before, the ZSF1 Obese animal model for HFpEF has already been described and is widely used by our group. While it is true that most HFpEF comorbidities were already studied in this model, hypothyroidism remained elusive. Preliminary results, in humans (data not shown) seemed to corroborate the incidence of hypothyroidism in some HFpEF patients, so we set out to preliminary investigate the TH axis in the ZSF1 model. To our surprise, preliminary results (see supplementary materials, Figure 13) showed that this rat model also presented lower T3 levels at twenty weeks of age, opening the possibility of studying the thyroid axis and the potential of its modulation as a therapeutic option on this model.

The major limitation that this model suffers from is the lack of fibrotic accumulation usually seen in HFpEF patients. In this specific study however, the impact of this limitation is highly diminished, as it was already proven that T3 prevents collagen deposition[30], thus, any functional improvements seen with the therapy could, potentially, be even greater if this factor was present.

Lastly, it is important to point out that our previous results (Chapter 3) shown that, while T3 therapy was able to decrease body, liver and fat weight, these values did not reach CT values. This reduction was expected, given the catabolism-inducing nature of the hormone, while the inability to reach CT levels was also foreseen given the lack of functional leptin receptors in the ZSF1 Obese model.

6.2 Animal model - experimental outcomes

T3 levels were found to be depressed in HFpEF rats versus CT. While we were unable to follow the hormone serum levels until the sacrifice, the trend seems steady, so alterations towards the end were unlikely. Nevertheless, further studies will be needed to confirm this.

Furthermore, as we have seen before, T4 and T3 can be locally degraded, so theoretically, TH levels can be even lower at the myocardium level than in the serum. This seems to be the case in our model, as our preliminary results shown a local significant decrease in the LV. For example, in a report by Weltman et al (2014), cardiac T4 and T3 levels were found to be altered with no significant differences in serum levels[64]. This shall be confirmed for the animal model used in this dissertation.

T3 supplemented rats displayed no evident alterations from vehicle treated HFpEF rats by the fifteenth week, two weeks after the beginning of the supplementation, with 0.04 µg/ml. This led us to increase T3 administration to 0.06 µg/ml, in an attempt to pursue serum levels similar to those of CT rats. This did not, however, result in any alterations of serum T3 levels.

As expected, T3 supplemented rats experienced decreased T4 serum levels, most likely due to negative feedback. This feedback expectedly resulted in lower T4 and T3 production by the thyroid, which in turn might have undermined the T3 increase via supplementation. Anyhow,

this T4 decline means that the administered T3 is producing some effect on the thyroid axis. TSH levels remained unaltered between groups, but importantly never completely fell to zero.

Combined, these results indicate a state of non-thyroidal illness in HFpEF rats. While the thyroid is functionally unaltered and unaffected, peripheral degradation of T4 and T3 led to low systemic levels. While, T3 supplementation did not seem to be sufficient to overcome this serum low-T3 state, as demonstrated in the results, the functional changes as a result of the therapy are undeniable (see chapter 3: [3.2]). These changes, in the absence of serum T3 alterations, might stem from the transient peaks in T3 at the time of water ingestion. Some of the freshly absorbed T3 can be internalized into the myocardium and immediately exert its function by escaping premature inactivation via D3. This hypothesis helps to explain the reason for these seemingly paradoxical results, but further studies will be necessary to confirm this.

Considering the preliminary results that showed decreased local and systemic levels of TH, the results derived from morphometric studies, echocardiography and hemodynamic support the functional changes assessed in single cardiomyocytes. Morphometrics studies revealed that T3 supplementation decreased obesity and attenuated diabetes metabolic abnormalities, thus eliminating some of the common comorbidities underlying HFpEF onset and progression. Furthermore, echocardiography and hemodynamic analysis, found several systolic and diastolic cardiac functional parameters to be ameliorated. Vascular function, as measured by arterial elastance, was also found to be significantly improved, likely due to its vasodilatation properties that increase aortic compliance[65]. When coupled with the reduction in end-diastolic pressure, these last two results indicate an important improvement in ventricular-arterial coupling.

One topic that warrants some discussion is the mortality we had in this model. Out of eight rats selected for T3 therapy, three died, while none of the other groups experienced any mortality. This was, likely due to the pro-arrhythmogenic effects of an excessive dose of T3 in the treated animals as further confirmed by the visual perception of slight arrhythmias on terminal hemodynamic evaluation (data not quantified). Future studies with a lower dose of T3 and telemetric monitoring will certainly result in decreased mortality with the same beneficial effects.

6.3 Isolated cardiomyocyte results

HFpEF patients are known for their diastolic dysfunction and recently there has been an increasing awareness that systolic dysfunction, albeit mild in comparison to HFrEF, is also present.

Cardiomyocytes derived from HFpEF rats presented significant delays in Ca^{2+} kinetics, which translated in delays in both contraction and relaxation, accompanied by impaired inotropism. The prolongation observed in the half-width of the contraction events may indicate diastolic dysfunction and could be one of the possible causes of exercise intolerance already described in the ZSF1 Ob animals[28]. All of these results provide an additional layer of knowledge

regarding HFpEF pathophysiology, namely at the level of intrinsic cardiomyocyte dysfunction. Interestingly, there was a very recent report by Smail et al (2018) of similar impairments in systolic and diastolic function on a diabetic rat model[59], one of the comorbidities present in the ZSF1 obese rats. Furthermore, another diabetic rat model has been reported to have anatomically specific hypothyroidism in the myocardial tissue[64], as a result of increased D3 expression. Since ZSF1 obese rats present diabetes, the possibility arises that the same expression of D3 occurs in the HFpEF model and, if true, might constitute another argument in favor of the impact of comorbidities as determinants of HFpEF.

At the cellular level, T3 treatment effectively reverted some of the functional hallmarks of HFpEF. Impaired Ca^{2+} kinetics were improved, as was the contractile capacity, measured by shortening amplitude. In this case however, the timings were slightly decreased even further than control. This is not entirely odd considering the cardiac effects that T3 has been reported to have, namely, upregulation of SERCA2, β-adrenergic receptors, voltage-gated K^+ channels, Na^+/K^+ ATPase and α/β-MHC, downregulation of phospholamban (PLB) and improvement of bioenergetics. All of these, altering the reactivity to *stimuli* and contractile kinetics (Figure 10). Our results did show a trend towards lower Ca^{2+} influx in HFpEF+T3, while maintaining identical contractile function to CT, hinting at the possibility of increased Ca^{2+} sensitivity, that the factors enumerated above could help to elucidate. If true, this could explain the increased kinetics, however, this condition can also suggest that local T3 levels were significantly higher than in CT, further fueling the notion that T3 was likely overdosed. Further studies in skinned cardiomyocytes and of myocardial quantification of TH are necessary to clarify this issue.

The diastolic phase of the cardiac cycle is a two-step process: The first, isovolumetric relaxation of the ventricle, is an energy-dependent active phase, highly dependent on some of the transporters mentioned above such as SERCA2A and PLB. Meanwhile, the second phase, linked to ventricular filling, is a passive phase that relies on the intrinsic compliance of the muscle fibers[66]. Our results indicate that the first portion of relaxation is fastest in treated rats and slowest in HFpEF, when compared to CT, while full relaxation is indeed slower in HFpEF, with no significant difference between CT and HFpEF, as measured by single exponential Tau.

This came as highly exciting, as it allowed us to further puzzle together some of the possible underlying mechanisms of relaxation in our experimental model, but inevitably raising more questions than answers. Slower relaxation times during the active phase in the HFpEF group are consistent with repressed Ca^{2+} clearance, while T3-induced overactivity in the treated rats resulted in lower relaxation times dependent on the Ca^{2+} transporters. In this regard, future studies of protein expression will allow us to uncover the players responsible for these alterations.

As for the second phase, while we are currently unable to isolate its contribution in the relaxation dysfunction, an inference can possibly be made from previous another study. It is known that HFpEF is associated to LV concentric hypertrophy. Our model, ZSF1 Obese, has also shown to have LV remodeling by 20 weeks of age and studies carried out in our lab have revealed a reduction in Sl_{max} of skinned cardiomyocytes from ZSF1 obese when compared to control (data not shown). Remarkably, we uncovered with this study that the chronical effect

of LV hypertrophy is already visible at the cellular level in the reduction of basal sarcomere length in unloaded cells. This further proves that possible compensatory structural remodeling is already undergoing, affecting the contractile machinery of the cardiomyocytes. After all, once we remove external influences, such as the matrix, cardiomyocytes were still slower to contract, relax, had lower contraction capacity and lower basal sarcomere length. Nonetheless, studies of skinned cardiomyocyte and titin (isoforms and phosphorylation state) are required to validate this hypothesis.

It was also fascinating to observe that both the exponential Tau obtained from hemodynamics and single cardiomyocyte studies denoted significant relaxation dysfunction, giving further credit to these results.

Our results point towards the possibility that, at least in part, the impaired Ca^{2+} reuptake is to blame, since cytoplasmic levels remain above the baseline long after peak contraction occurred. Impaired Ca^{2+} reception can lead to its cytoplasmic accumulation, as was seen at higher frequencies in untreated HFpEF rats, with no influence in transient amplitudes. This is important since rats have a physiological heart rate around 7Hz, suggesting that this might constitute another pathophysiological mechanism for heart failure in this model. In the long run, the Ca^{2+} accumulation can lead to cardiac dysfunction via reactive oxygen species (ROS) that can further perpetuate the cytoplasmic Ca^{2+} overload through changes in L-type channel mediated influx and efflux by Ca^{2+} ATPase[67,68]. Furthermore, Ca^{2+} is known to have an impact in gene regulation and activation of phospholipases that invariably can lead to subcellular remodeling and aggravate cardiac dysfunction[68]. T3 therapy shown to be effective at decreasing this cytoplasmic accumulation, most likely due to its aforementioned effects on the activation of SERCA2 and repression of PLB.

Lastly, while we cannot attribute with certainty the heft of each individual improvement, the results we obtained so far are simply not circumscribed to the heart, but revealed metabolic benefits. The wide range of changes comes as no surprise when fiddling with a hormonal axis, but it certainly seems fitting to use such a complex physiological mechanism to fight such an intricate and multifactorial pathology.

6.4 Methodology

Cardiomyocytes are known for their state of terminal differentiation, inability to divide and tight adherence with the cardiac matrix and other cardiomyocytes. These nuances make researching primary cardiomyocytes an intricate task. Any experimental procedure that makes use of isolated cardiomyocytes is constrained by the amount of rod-shaped, calcium tolerant cardiomyocytes that are successfully isolated, so careful optimization of this method is required for efficient isolation given its status as a determining step for the success of the technique[62].

The preferred protocol for cardiac isolation is retrograde coronary perfusion (RCP) with enzyme solution, although other types of isolation procedures have been tried and reported, till this day, the yield obtained from these alternative methods are modest in comparison to

RCP. A good review on this topic that can help to implement, troubleshoot and improve the isolation procedure has been published by Louch, (2011) *et al*. [69].

In this experiment we used RCP for the isolation using a Ca^{2+}-free collagenase solution but, unlike most protocols, we removed the apex of the heart before perfusion. This allowed us to save a considerable amount of cardiac sample for molecular and biochemical studies, without compromising the final isolation yield significantly. However, care should be taken in opting for this alteration, since backpressure is important for efficient perfusion, enzyme delivery and, consequentially, for collagen matrix digestion and cardiomyocyte isolation.

For the present experimental setting, contraction and Ca^{2+} transient measurements were recorded using the IonOptix system we recently implemented in our laboratory. This technique allowed us to obtain large amounts of data with considerably low deviation between cells from a specimen and within the specimen group itself. As was already hinted at before, this technique is of great experimental value since the researcher can fully control the ambient and conditions the isolated cardiomyocytes are exposed to, while still obtaining reliable functional data from a considerable amount of cells/sample.

In our experimental design we kept the conditions as close to physiological as possible, using Tyrode's buffer that is known to be a good medium for functional studies, with temperature controlled at a physiologic 37^{o}C. At this point an argument can be made in regard to the lack of a matrix simulating the conditions the cardiomyocytes are subjected to *in vivo* by the extracellular matrix. This became evident in the resting sarcomere length that averaged around 1.80 µm in our experimental conditions, which is significantly shorter than the length at which maximum isometric tension is produced (L_{max}), reported to be around 2.2µm[70]. The matrix and interaction with other cardiomyocytes creates a permanent passive tension that is not represented in this technique. But, while it is true that contraction capacity is different depending on the rigidity of the substrate, as recently published by our group[71], in this study we set out to find the effects of T3 supplementation by direct comparison, so introducing another variable or source of confusion could potentially undermine the differences we observed in our results.

Another case can, potentially, be made for the addition of T3 in the medium in an appropriate concentration to mimic the serum levels present in each specific group. While this would make some sense from a theoretical standpoint, this has however, some limitations. As mentioned before (see Introduction, Figure 3), cardiac T3 levels can differ from serum levels, so proper matching would be difficult given the time incompatibility between receiving the ELISA results and transient measurements. On the other hand, the lack of T3 in the media allowed us to forgo any changes associated to acute effects of T3 and obtain functional data from the long-lasting alterations of prolonged T3 supplementation *in vivo.*

Chapter 7

Conclusions and Future Perspectives

To this day, HFpEF remains a very frequent and troubling disease with no effective therapy posing a massive clinical problem.

In this project, we were able to collect promising data on diverse functional benefits that preemptive oral T3 therapy had on the development of HFpEF in a rat model that exhibits several comorbidities akin to those usually found in HFpEF patients such as obesity, diabetes, hypertension and local hypothyroidism, but the certainty of an overdose that led to some adverse effects prevents immediate translation to the clinical setting without further studies. As such, future studies with lower dosage and alternative delivery methods are already planned. That does not however subtract from the validity of the results obtained, as the advantages detected in isolated cardiomyocytes were clear: both inotropic, but more importantly, lusitropic function were recovered. Relaxation delays, that are one of the hallmarks of HFpEF, were effectively nullified and intracellular Ca^{2+} accumulation at higher stimulation frequencies was reversed. From a mechanistic standpoint it will be interesting to further study and confirm the pathways and regulations involved in these benefits so we intend to probe the heart tissue samples for several proteins (Supplementary Material: Table 8) using RT-PCR and western-blot. It is worth mention the importance that evaluating the expression of the different types of deiodinases, but most notably of D3, will have, since, to the best of my knowledge, there is no experimental data on the alterations of the levels of these specific proteins in any model of HFpEF.

An added benefit of using T3 as a therapeutic tool for HFpEF is the sheer amount of pharmacological data already available since it is already a Food and Drug Administration (FDA) approved drug, thus making potential future clinical studies easier.

The clear step moving forward will, undoubtedly, be to repeat the study with lower T3 prescription. Some further consideration will be given in the delivery method since fluid intake can vary substantially and subsequently affecting the daily T3 dosage. Additionally, a bigger sample size will be used to avoid precluding statistical significance, as was likely the case in some echocardiographic and hemodynamic parameters. In the isolated myocyte technique, as was discussed before, the possibility of including a heart stiffness matched matrix in the measurements will be considered, as will the supplementation of the medium with a matched T3 concentration, even though technical difficulties might hinder these additions.

Chapter 8

References

1. Benjamin, E. J. *et al. Heart Disease and Stroke Statistics-2017 Update: A Report from the American Heart Association*. *Circulation* **135,** (2017).

2. Organization, W. H. *Global status report on noncommunicable diseases*. (2010).

3. Bui, A. L., Horwich, T. B. & Fonarow, G. C. Epidemiology and risk profile of heart failure. *Nat. Rev. Cardiol.* **8,** 30–41 (2011).

4. Ponikowski, P. *et al.* 2016 ESC Guidelines for the diagnosis and treatment of acute and chronic heart failure. *Eur. Heart J.* **37,** 2129–2200 (2016).

5. Hamdani, N. *et al.* Myocardial titin hypophosphorylation importantly contributes to heart failure with preserved ejection fraction in a rat metabolic risk model. *Circ. Hear. Fail.* **6,** 1239–1249 (2013).

6. Fontes-carvalho, R. & Leite-moreira, A. Heart Failure with Preserved Ejection Fraction : Fighting Misconceptions for a New Approach. *Arq. Bras. Cardiol.* **96,** 504–513 (2011).

7. Bhatia, R. S. *et al.* Outcome of Heart Failure with Preserved Ejection Fraction in a Population-Based Study. *N. Engl. J. Med.* **355,** 260–269 (2006).

8. Tribouilloy, C. *et al.* Prognosis of heart failure with preserved ejection fraction: a 5 year prospective population-based study. *Eur. Heart J.* **29,** 339–347 (2008).

9. Paulus, W. J. & van Ballegoij, J. J. M. Treatment of Heart Failure With Normal Ejection Fraction. *J. Am. Coll. Cardiol.* **55,** 526–537 (2010).

10. Leite, S. *et al.* Echocardiography and invasive hemodynamics during stress testing for diagnosis of heart failure with preserved ejection fraction: an experimental study. *Am. J. Physiol. - Hear. Circ. Physiol.* **308,** H1556–H1563 (2015).

11. Empel, V. Van & Rocca, H. B. Inflammation in HFpEF : Key or circumstantial? *Int. J. Cardiol.* **189,** 259–263 (2015).

12. Dougherty, A. H., Naccarelli, G. V, Gray, E. L., Hicks, C. H. & Goldstein, R. A. Congestive Heart Failure with Normal Systolic Function. *Am. J. Cardiol.* **54,** 778–782 (1984).

13. Owan, T. E. *et al.* Trends in Prevalence and Outcome of Heart Failure with Preserved Ejection Fraction. *N. Engl. J. Med.* **355,** 251–259 (2006).

14. Greene, S. J. *et al.* The cGMP Signaling Pathway as a Therapeutic Target in Heart Failure With Preserved Ejection Fraction. *J. Am. Heart Assoc.* **2,** e000536–e000536 (2013).

15. Borlaug, B. A., Lam, C. S. P., Roger, V. L., Rodeheffer, R. J. & Redfield, M. M. Contractility and Ventricular Systolic Stiffening in Hypertensive Heart Disease. *J. Am. Coll. Cardiol.* **54,** 410–418 (2009).

16. Leite-Moreira, A. F. Current perspectives in diastolic dysfunction and diastolic heart failure. *Heart* **92,** 712–8 (2006).

17. Lam, C. S. P., Donal, E., Kraigher-Krainer, E. & Vasan, R. S. Epidemiology and clinical course of heart failure with preserved ejection fraction. *Eur. J. Heart Fail.* **13,** 18–28 (2011).

18. De Keulenaer, G. W. & Brutsaert, D. L. Systolic and Diastolic Heart Failure Are Overlapping Phenotypes Within the Heart Failure Spectrum. *Circulation* **123,** 1996–2005 (2011).

19. Packer, M. Can Brain Natriuretic Peptide Be Used to Guide the Management of Patients With Heart Failure and a Preserved Ejection Fraction?: The Wrong Way to Identify New Treatments for a Nonexistent Disease. *Circ. Hear. Fail.* **4,** 538–540 (2011).

20. Shah, S. J. & Gheorghiade, M. Heart Failure With Preserved Ejection Fraction: treat now by treating comorbidities. *JAMA* **300,** 431 (2008).

21. Mohammed, S. F. *et al.* Comorbidity and ventricular and vascular structure and function in heart failure with preserved ejection fraction: a community-based study. *Circ. Heart Fail.* **5,** 710–9 (2012).

22. Sharma, K. & Kass, D. A. Heart failure with preserved ejection fraction: Mechanisms, clinical features, and therapies. *Circ. Res.* **115,** 79–96 (2014).

23. Zile, M. R. *et al.* Myocardial stiffness in patients with heart failure and a preserved ejection fraction contributions of collagen and titin. *Circulation* **131,** 1247–1259 (2015).

24. Van Heerebeek, L. *et al.* Diastolic stiffness of the failing diabetic heart: Importance of fibrosis, advanced glycation end products, and myocyte resting tension. *Circulation* **117,** 43–51 (2008).

25. Falcao-Pires, I. *et al.* Diabetes Mellitus Worsens Diastolic Left Ventricular Dysfunction in Aortic Stenosis Through Altered Myocardial Structure and Cardiomyocyte Stiffness. *Circulation* **124,** 1151–1159 (2011).

26. Canaris, G. J., Tape, T. G. & Wigton, R. S. Thyroid disease awareness is associated with high rates of identifying subjects with previously undiagnosed thyroid dysfunction. *BMC Public Health* **13,** 351 (2013).

27. Senthil Selvaraj, Irwin Klein, Sara Danzi, Nausheen Akhter, R. O. & Bonow and Sanjiv J. Shah, M. Association of Serum Triiodothyronine with B-type Natriuretic Peptide and Severe Left Ventricular Diastolic Dysfunction in Heart Failure with Preserved Ejection Fraction. *Am J Cardiol.* **110,** 234–239 (2012).

28. Conceição, G., Heinonen, I., Lourenço, A. P., Duncker, D. J. & Falcão-Pires, I. Animal models of heart failure with preserved ejection fraction. *Neth. Heart J.* **24,** 275–286 (2016).

29. Ord, W. M. On Myxœdema, a term proposed to be applied to an essential condition in the "Cretinoid" Affection occasionally observed in Middle-aged Women. *Med. Chir. Trans.* **61,** 57–78.5 (1878).

30. Jabbar, A. *et al.* Thyroid hormones and cardiovascular disease. *Nat. Rev. Cardiol.* **14,** 39–55 (2016).

31. Murray, G. R. Note on the Treatment of Myxoedema by Hypodermic Injections of an Extract of the Thyroid Gland of a Sheep. *Br. Med. J.* **2,** 796–7 (1891).

32. Yazici, M. *et al.* Effects of thyroxin therapy on cardiac function in patients with subclinical hypothyroidism: Index of myocardial performance in the evaluation of left ventricular function. *Int. J. Cardiol.* **95,** 135–143 (2004).

33. Dillmann, W. H. Biochemical basis of thyroid hormone action in the heart. *Am. J. Med.* **88,** 626–630 (1990).

34. Danzi, S. & Klein, I. Thyroid Hormone-Regulated Cardiac Gene Expression and Cardiovascular Disease. *Thyroid* **12,** 467–472 (2002).

35. Simonides, W. S. *et al.* Hypoxia-inducible factor induces local thyroid hormone inactivation during hypoxic-ischemic disease in rats. *J. Clin. Invest.* **118,** 975–83 (2008).

36. Degroot, L. J. in *Endotext* 1–35 (MDText.com, Inc., 2015).

37. Visser, T. J. in *Endotext* **4,** 1–20 (MDText.com, Inc., 2016).

38. Meuwese, C. L., Dekkers, O. M., Stenvinkel, P., Dekker, F. W. & Carrero, J. J. Nonthyroidal illness and the cardiorenal syndrome. *Nature Reviews Nephrology* **9,** 599–609 (2013).

39. Holt, R. I. G., Hanley, N. A. & Brook, C. G. D. (Charles G. D. *Essential endocrinology and diabetes.* (Blackwell Pub, 2007).

40. Ascheim, D. D. & Hryniewicz, K. Thyroid Hormone Metabolism in Patients with Congestive Heart Failure: The Low Triiodothyronine State. *Thyroid* **12,** 511–515 (2002).

41. Klein, I. & Danzi, S. Thyroid Disease and the Heart. *Circulation* **116,** 1725–1735 (2007).

42. Selvaraj, S. *et al.* Association of serum triiodothyronine with B-type natriuretic peptide and severe left ventricular diastolic dysfunction in heart failure with preserved ejection fraction. *Am. J. Cardiol.* **110,** 234–9 (2012).

43. Pingitore, A. & Iervasi, G. Thyroid (dys)function in heart failure: is it a potential target for medical treatment? *Vasc. Health Risk Manag.* **1,** 97–100 (2005).

44. Iacoviello, M. *et al.* Prognostic Role of Sub-Clinical Hypothyroidism in Chronic Heart Failure Outpatients. *Curr. Pharm. Des.* **14,** 2686–2092 (2008).

45. Roth, G. M., Bader, D. M. & Pfaltzgraff, E. R. Isolation and physiological analysis of mouse cardiomyocytes. *J. Vis. Exp.* e51109 (2014).

46. Ravens, U. Cardiac mechano-electric coupling research: Fifty years of progress and scientific innovation. *Prog. Biophys. Mol. Biol.* **115,** 71–75 (2014).

47. Jourdon, P. & Feuvray, D. Calcium and potassium currents in ventricular myocytes isolated from diabetic rats. *J. Physiol.* **470,** 411–429 (1993).

48. Beuckelmann, D. J., Näbauer, M. & Erdmann, E. Alterations of K+ currents in isolated human ventricular myocytes from patients with terminal heart failure. *Circ. Res.* **73,** 379–85 (1993).

49. Crespo, L. M., Grantham, C. J. & Cannell, M. B. Kinetics, stoichiometry and role of the Na–Ca exchange mechanism in isolated cardiac myocytes. *Nature* **345,** 618–621 (1990).

50. Beuckelmann, D. J., Näbauer, M. & Erdmann, E. Characteristics of calcium-current in isolated human ventricular myocytes from patients with terminal heart failure. *J. Mol. Cell. Cardiol.* **23,** 929–937 (1991).

51. Kennedy, D. *et al.* Effect of chronic renal failure on cardiac contractile function, calcium cycling, and gene expression of proteins important for calcium homeostasis in the rat. *J. Am. Soc. Nephrol.* **14,** 90–7 (2003).

52. Schwinger, R. H. *et al.* The failing human heart is unable to use Frank Starling's mechanism. *Circ.Res.* **74,** 959–969 (1994).

53. Silver, R. B. Ratio imaging: measuring intracellular Ca++ and pH in living cells. *Methods Cell Biol.* **72,** 369–87 (2003).

54. Grynkiewicz, G., Poenie, M. & Tsien, R. Y. A new generation of Ca2+ indicators with greatly improved fluorescence properties. *J. Biol. Chem.* **260,** 3440–3450 (1985).

55. Borges Canha, M. *et al.* Characterization of liver changes in ZSF1 rats, an animal model of metabolic syndrome. *Rev. Esp. Enferm. Dig.* **109,** 491–497 (2017).

56. Falcão-Pires, I. *et al.* Distinct mechanisms for diastolic dysfunction in diabetes mellitus and chronic pressure-overload. *Basic Res. Cardiol.* **106,** 801–814 (2011).

57. MCCROSSAN, Z., Billeter, R. & White, E. Transmural changes in size, contractile and electrical

properties of SHR left ventricular myocytes during compensated hypertrophy. *Cardiovasc. Res.* **63,** 283–292 (2004).

58. Pohlmann, L. *et al.* Cardiac myosin-binding protein C is required for complete relaxation in intact myocytes. *Circ. Res.* **101,** 928–938 (2007).

59. Manal *et al.* Voltage dependence of the Ca 2+ transient in endocardial and epicardial myocytes from the left ventricle of Goto–Kakizaki type 2 diabetic rats. *Mol. Cell. Biochem.* **103,** 502–511 (2018).

60. Hongo, K., Kusakari, Y., Konishi, M., Kurihara, S. & Mochizuki, S. Estimation of myofibrillar responsiveness to Ca2+ in isolated rat ventricular myocytes. *Eur. J. Physiol.* 639–645 (1998).

61. Pasqualin, C. *et al.* SarcOptiM for ImageJ: high-frequency online sarcomere length computing on stimulated cardiomyocytes. *Am. J. Physiol. Physiol.* **311,** C277–C283 (2016).

62. Schlüter, K.-D. & Schreiber, D. in *Basic Cell Culture Protocols* (eds. Helgason, C. D. & Miller, C. L.) **290,** 305–314 (Humana Press Inc., Totowa, Nj, 2004).

63. Voigt, N., Zhou, X.-B. & Dobrev, D. Isolation of Human Atrial Myocytes for Simultaneous Measurements of Ca^{2+} Transients and Membrane Currents. *J. Vis. Exp.* 1–9 (2013).

64. Weltman, N. *et al.* Low-dose T_3 replacement restores depressed cardiac T_3 levels, preserves coronary microvasculature and attenuates cardiac dysfunction in experimental diabetes mellitus. *Mol. Med.* **20,** 302–312 (2014).

65. Samuel, S., Zhang, K., Tang, Y. Da, Gerdes, A. M. & Carrillo-Sepulveda, M. A. Triiodothyronine potentiates vasorelaxation via pkG/VASP signaling in vascular smooth muscle cells. *Cell. Physiol. Biochem.* **41,** 1894–1904 (2017).

66. Saini, H., Tabtabai, S., Stone, J. R. & Ellinor, P. T. in *Cellular and Molecular Pathobiology of Cardiovascular Disease* 101–119 (Elsevier, 2014).

67. Touyz, R. M. Reactive Oxygen Species as Mediators of Calcium Signaling by Angiotensin II: Implications in Vascular Physiology and Pathophysiology. *Antioxid. Redox Signal.* **7,** 1302–1314 (2005).

68. Jugdutt, B. I. & Dhalla, N. S. *Cardiac remodeling : molecular mechanisms*. (Springer, 2013).

69. Louch, W. E., Sheehan, K. A. & Wolska, B. M. Methods in Cardiomyocyte Isolation, Culture, and Gene Transfer. *J Mol Cell Cardiol.* **51,** 288–298 (2011).

70. Verduyn, S. C., Zaremba, R., van der Velden, J. & Stienen, G. J. M. Effects of contractile protein phosphorylation on force development in permeabilized rat cardiac myocytes. *Basic Res. Cardiol.* **102,** 476–87 (2007).

71. van Deel, E. D. *et al.* In vitro model to study the effects of matrix stiffening on Ca 2+ handling and myofilament function in isolated adult rat cardiomyocytes. *The Journal of Physiology* **595,** 4597–4610 (2017).

Chapter 9

Supplementary material

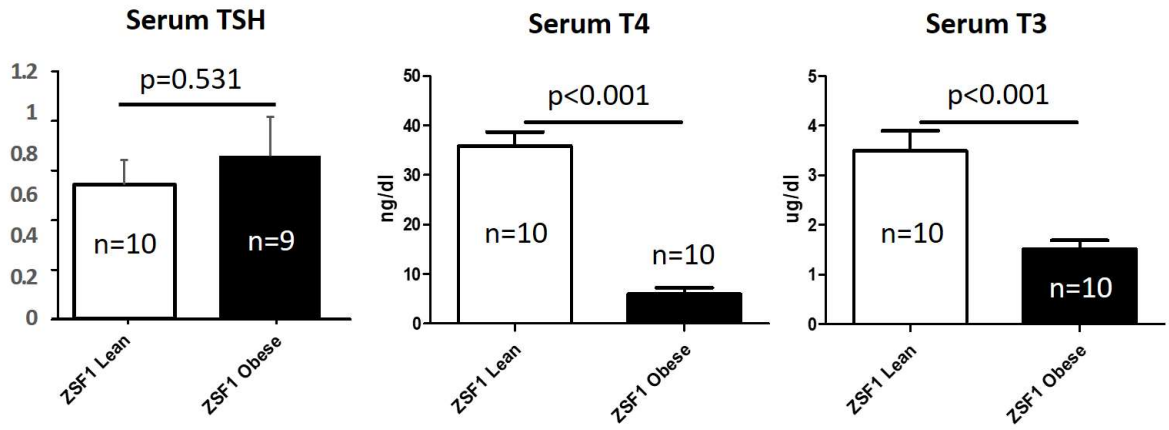

Figure 13: Preliminary results: changes in serum thyroid hormones were present in the ZSF1 Obese model of HFpEF.

Table 6 – Number of serum samples analyzed by week, group and hormone

	Weeks	13	15	17	19
CT	T3	5	5	5	4
	T4	5	5	5	5
	TSH	5	5	5	5
HFpEF	T3	8	8	8	8
	T4	8	8	8	8
	TSH	8	8	8	8
HFpEF+T3	T3	8	8	7	6
	T4	8	8	7	7
	TSH	8	7	7	7

Table 7 – Formulations for the buffers used in the cardiomyocyte isolation procedure

Digestion Buffer	Concentration (mM)	Ref
NaCl	130	1.06404 Merck
KCl	5.4	1.04936 Merck
Pyruvate	3	P2256 Sigma
HEPES	25	H3375 Sigma
$MgCl_2.6H_2O$	0.5	1.05833 Merck
$NaH_2PO_4.H_2O$	0.33	1.06345 Merck
Glucose	22	1.08337 Merck
Tyrode's Buffer	**Concentration (mM)**	**Ref**
NaCl	133.5	1.06404 Merck
KCl	5.0	1.04936 Merck
$NaH_2PO_4.H_2O$	1.2	1.06345 Merck
$MgSO_4$	1.2	1.05886 Merck
HEPES	10	H3375 Sigma
Glucose	11	1.08337 Merck

Table 8 – Proteins of interest for future RT-PCR and western blot analysis

Proteins of interest
SERCA
Phospholamban
Deiodinase type 1-3
Thyroid hormone receptors: TRα1, TRα2, TRβ1
Myosin heavy chain: α-MHC, β-MHC
RYR2, Na+/Ca2+ exchanger
Nitric oxide synthase
Natriuretic peptide precursor B (Nppb)
HIF-1α
B-type natriuretic peptide
Titin

Extended methodology for the previous results

Metabolic studies

Following 12 hours of fasting period, the animals were submitted to oral glucose-tolerance and IR tests. Glycaemia was assessed after 15, 30, 60, 90 and 120 minutes following the administration of glucose (1 $g.Kg^{-1}$) and insulin (0.5 $U.Kg^{-1}$) by gavage and intraperitoneal injection, respectively.

Echocardiography

Animals were anaesthetized by inhalation of sevoflurane (8% for induction and 1-2.5% for maintenance), endotracheally intubated and mechanically ventilated (150 min−1, 100% O_2, 14–16 cmH_2O inspiratory pressure, with tidal volume adjusted to animal weight, and 4 cmH_2O end-expiratory pressure) (TOPO Small Animal Ventilator, Kent Scientific Inc., USA). Rats were placed in a left-lateral decubitus position on a heating pad, the ECG was monitored and their temperature was kept at 38°C. Two-dimensionally (2D)-guided M-mode echocardiography and pulse-wave Doppler echocardiography were performed using an echocardiographic system equipped with a 15-MHz linear-transducer (Sequoia 15L8W), and the exams were performed with the animals placed over a heating pad, in the prone left lateral decubitus position with a full chest shaving.

Parasternal long-axis images of the aorta, LA and LV were first obtained; 90° rotation from the long-axis view produced a short axis view of the heart. M-Mode short-axis view at the level of the papillary muscle was used to assess wall thickness as well as systolic and diastolic left ventricular cavity dimensions. The following Doppler and tissue Doppler measurements were taken using the apical four-chamber early diastolic filling peak velocity (E wave), late diastolic peak velocity (A wave), E/A ratio, isovolumetric relaxation time (IVRT), isovolumetric contraction time (IVCT), early peak diastolic filling velocity (E'), late peak diastolic filling velocity (A') and mitral annular systolic velocity (S'). Three representative cycles were measured per rat and their average was calculated.

Hemodynamic instrumentation

After intraperitoneal sedation by a mixture of fentanyl and midazolam (100 $\mu g.kg^{-1}$ and 5 $mg.kg^{-1}$, respectively), rats were anaesthetized (with a mixture of 8% and 1-2.5% sevoflurane with oxygen for induction and support, respectively), endotracheally intubated, (mechanically ventilated (150 min^{-1}, 100% O_2, 14–16 cmH_2O inspiratory pressure, with tidal volume adjusted to animal weight, and 4 cmH2O end-expiratory pressure; TOPO Small Animal Ventilator, Kent Scientific Inc.) and placed over a heating pad (38°C).

To compensate for perioperative fluid losses, the femoral vein was cannulated and warm Ringer lactate's solution fluid was administered with a perfusion pump (Multi-Phaser™, NE-1000, New Era Pump Systems). Under surgical microdissection (Wilde M651, Leica microsystems), left thoracotomy was performed, pericardium was widely opened and pressure–volume (PV) catheters were implanted through the apex along the LV (SPR-838 and PVR-1045, Millar Instruments, Houston, TX, respectively). After 15 min of stabilization, recordings were done at the end-expiration under basal conditions and transient inferior vena cava and aortic occlusions in order to assess pressure-volume relations. The systemic blood pressure was recorded by advancing the left ventricle catheter to the aorta. Parallel conductance and field inhomogeneity were estimated by 50µL 10% saline injections and CO measurement (Perivascular Flowmeter Module, AD Instruments Technology), respectively. Data were continuously acquired (MPVS 300, Millar Instruments), digitally recorded at 1000 Hz (ML880 PowerLab 16/30, Millar Instruments), and analyzed (PVAN 3.5™, Millar Instruments). Heart rate, stroke volume, end-diastolic volume (EDV), end-systolic volume (ESV), EF, end-diastolic pressure (EDP) and end-systolic pressure (ESP) were determined from the pressure–volume tracings. Effective systemic arterial elastance (EA), as a measure of LV afterload, was calculated dividing ESP by SV. Relaxation rate was estimated with the time constant τ using the Glantz method.